

AD-A135 248

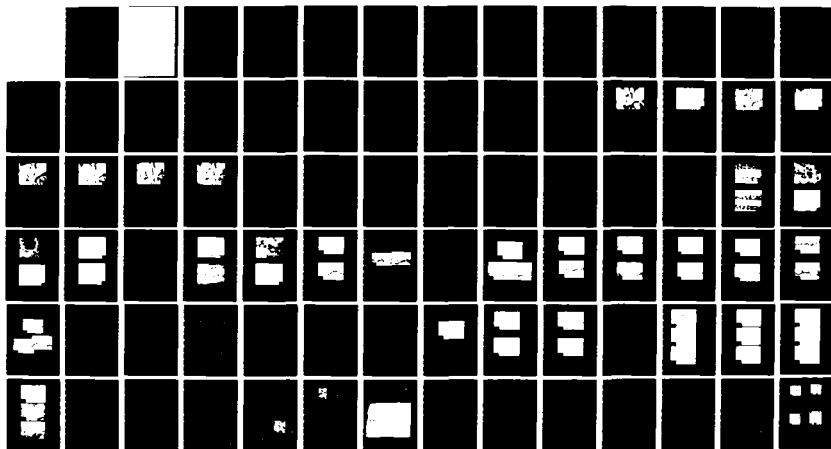
DISCLINATIONS IN CARBON-CARBON COMPOSITES(U) ACUREX
CORP/AEROTHERM MOUNTAIN VIEW CA J E ZIMMER ET AL.
SEP 83 TR-83-21/ATD N00014-81-C-0641

1/1

UNCLASSIFIED

F/G 11/4

NL

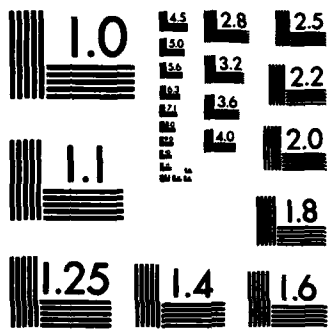


END

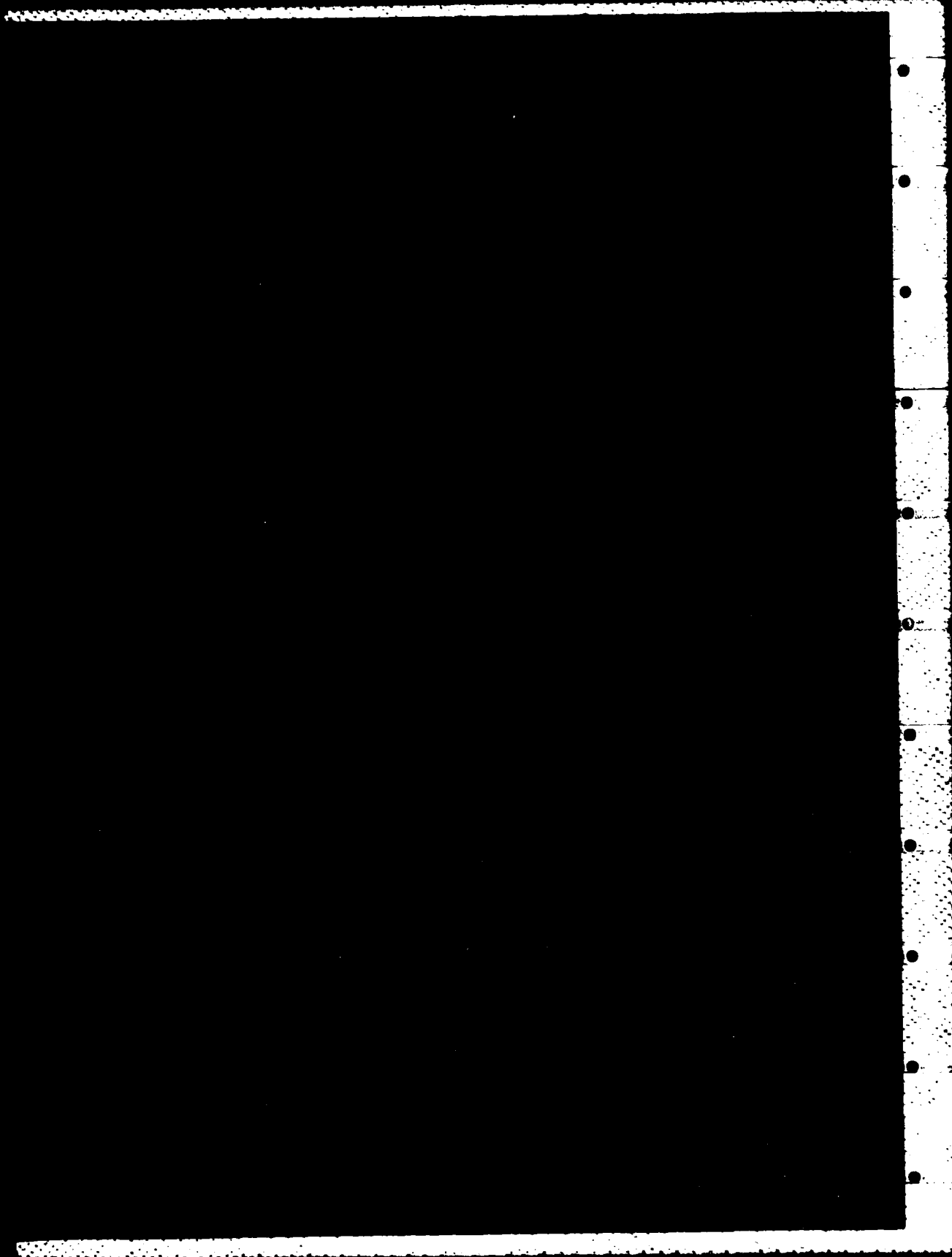
FILMED

104

DTIC



MICROCOPY RESOLUTION TEST CHART
NATIONAL BUREAU OF STANDARDS-1963-A



relationship of the disclinations to the fracture behavior of the composite matrix.

The three-dimensional structure of disclination arrays in the carbonaceous mesophase has been delineated by optical micrography on successive parallel planes of section. The disclinations intersected each plane of section, denoting a line character to the central core of the disclinations. This analysis showed that the disclination lines (cores) are generally curved and can interact by two disclinations joining to form a single disclination or by one disclination separating to form two disclinations. Disclination theory requires that for such disclination interactions, the total strength or rotation of the disclinations must be conserved. The evidence obtained in this study supports this requirement. This mapping of the three-dimensional structure of the disclination arrays provides a better insight into the complex microstructure of carbon-carbon composites.

The qualitative effect of disclinations on shear-type cracks in a carbon-carbon composite has been investigated. Shear cracks were introduced in a two-directional carbon-carbon composite by short-beam shear testing. This composite was a laminate of graphite-fiber fabric with a matrix from coal-tar pitch precursor. The shear cracks and their path through the graphite-fiber bundles were observed with optical and scanning electron microscopy. The crack path was controlled by the disclinations and was diverted or altered depending on the structure of the disclinations. The disclinations produced a tongue-and-groove type of fracturing; this tortuous fracturing is a mechanism for increased fracture toughness for carbon-matrix composites.

Further details of the core structure of the negative wedge disclinations in a graphite-fiber bundle have been obtained by scanning electron microscopy. This micrography distinguished between the discontinuous cores of disclinations of strength $S = -1/2$ and $S = -3/2$ and the continuous, saddle-like cores of the disclinations of strength $S = -1$ and $S = -2$.

FOREWORD

This is the second annual report on a program to study the disclinations in carbon-carbon composites. The work is supported by the Office of Naval Research under Contract N00014-81-C-0641. Dr. L. H. Peebles, Jr. is the Scientific Officer; his interest and support are gratefully acknowledged.

TABLE OF CONTENTS

	<u>Page</u>
INTRODUCTION	1
BACKGROUND	3
THREE DIMENSIONAL ARRAYS	11
SHEAR FRACTURE AND DISCLINATIONS IN A CARBON-CARBON COMPOSITE . . .	29
CORE STRUCTURE OF DISCLINATIONS	49
PUBLICATIONS	65
REFERENCES	76

LIST OF ILLUSTRATIONS

<u>Figure</u>		<u>Page</u>
1	Schematic model of the carbonaceous mesophase, a discotic nematic liquid crystal	4
2	Wedge disclinations in the carbonaceous mesophase	5
3	Twist disclinations in the carbonaceous mesophase	5
4	A Nabarro circuit about a wedge disclination	6
5	Reflectance of polarized light from a graphite crystal	8
6	Schematic diagram of micrographic technique for observing three-dimensional disclination arrays	13
7	Optical micrograph and structural sketch of disclination array in carbonaceous mesophase; first plane of section, cross-polarized light	15
8	Optical micrograph and structural sketch of same area as Figure 7 on second plane of section 5 μm below first plane	16
9	Optical micrograph and structural sketch on third plane of section, 10 μm below second plane	17
10	Optical micrograph and structural sketch on fourth plane of section, 8 μm below third plane	18
11	Optical micrograph and structural sketch on fifth plane of section, 5 μm below fourth plane	19
12	Optical micrograph and structural sketch on sixth plane of section, 5 μm below fifth plane	20
13	Optical micrograph and structural sketch on seventh plane of section, 8 μm below sixth plane	21
14	Optical micrograph and structural sketch on eighth plane of section, 5 μm below seventh plane	22
15	Sketch of the three-dimensional structure of the disclination array	24
16	Projection of disclination array containing interactions on vertical plane normal to planes of section	26
17	Sketches of disclination interactions on adjacent parallel planes of section	27

LIST OF ILLUSTRATIONS (Continued)

<u>Figure</u>		<u>Page</u>
18	Optical micrographs of shear cracks in two-dimensional carbon-carbon composite	31
19	Optical micrographs of shear cracks in fiber bundle near its edge	32
20	Optical micrographs of shear cracks in fiber bundle . . .	33
21	Optical micrographs of shear crack in fiber bundle . . .	34
22	Optical micrographs of shear crack at region between perpendicular fiber bundles	36
23	Optical micrographs of shear crack between filaments . .	37
24	Scanning electron micrographs of shear crack in two-directional carbon-carbon composite	38
25	Micrograph of same shear crack as in Figure 24	39
26	Micrographs of shear crack among graphite filaments . . .	41
27	Micrographs of shear crack showing angular fracture surfaces	42
28	Micrographs of shear crack near disclination of strength $S = -1$	43
29	Micrographs of shear crack showing angular fracture surface at disclinations of strength $S = -1/2$	44
30	Micrographs of shear crack with tongue-and-groove type of fracturing at the disclinations	45
31	Micrographs of shear crack at disclinations of strength $S = -1/2$	46
32	Micrograph of shear crack and $S = -1/2$ disclinations . .	47
33	Structure of wedge disclinations in arrays of filaments in a graphite-fiber bundle	50
34	Structure of continuous cores; adjacent surfaces would be stacked vertically along the disclination line	52
35	Scanning electron micrograph of disclination of strength $S = -1/2$ with discontinuous core	54

LIST OF ILLUSTRATIONS (Concluded)

<u>Figure</u>		<u>Page</u>
36	Micrographs of disclinations among fibers in square arrays; two disclinations of strength $S = -1/2$, $S = -1$ disclination	55
37	Wedge disclinations of strength $S = -1$ with continuous saddle core	56
38	Disclinations among fibers in pentagonal array of equivalent strength $S = -3/2$	58
39	Disclination of strength $S = -3/2$ pentagonal array . . .	59
40	Disclinations among fibers in hexagonal array of equivalent strength $S = -2$	60
41	Disclination of strength $S = -2$ in hexagonal array . . .	61
42	Schematic diagram of fracturing in a graphite-fiber bundle	63

INTRODUCTION

Disclinations are prominent in the microstructure of carbon-carbon composites, the principal material for thermal protection systems, such as rocket nozzles and reentry vehicle nosetips, and for high-temperature, structural components for turbine engines and tactical missiles. Disclinations are rotational elastic distortions in the graphite matrix of these composites introduced when the matrix was formed via the carbonaceous mesophase, a discotic nematic liquid crystal. The association of disclinations with the microstructure of carbon-carbon composites implies a relationship between the disclinations and the structure-sensitive physical properties of these composites. Thus, basic research is needed to not only understand the topological aspects of disclinations, but also to understand the disclination structures in carbon-carbon composites and the role of these disclinations in controlling the physical properties of these composites.

Carbon-carbon composites have graphitic matrices reinforced with high-strength, high-modulus graphite fibers from rayon, polyacrylonitrile or mesophase pitch. These composites exhibit some unique properties: their elastic modulus at room temperature is retained at elevated temperatures, their volumetric thermal expansion is quite low, and they have good fracture toughness. These properties exceed those of other ceramic materials with crystal lattices that do not contain disclinations. Disclinations are inherent in the carbon-carbon composites, since their microstructure is formed

during the transformation by pyrolysis of the matrix precursors such as petroleum and coal-tar pitches to the carbonaceous mesophase. Disclinations can exist in this liquid crystal because as the high rotational strains of the disclinations are reduced by flow of the oriented molecules of the liquid crystal.

The objectives of this basic research on the disclinations in carbon-carbon composites are to identify and classify the disclination structures in the matrix of carbon-carbon composites and to determine the relationship of the disclinations to the fracture behavior of the composite matrix.

The specific areas of research which are described in this report are the following: observation of the types and arrangement of disclinations in a disclination array in the carbonaceous mesophase; observation of shear fracture and its relation to disclinations in a carbon-carbon composite; and the characterization of the core structures of the disclinations in the matrix in a carbon-fiber bundle in a carbon-carbon composite.

Disclinations are discontinuities in the parallel stacking of the molecular layers of the graphitic matrix materials. The patterns involved in this parallel stacking with disclinations present resemble in a way the patterns of fingerprints. In the graphitic matrix, these patterns exist not on a surface (skin), but in three dimensions. This report identifies these complex patterns and characterizes the effect of the disclinations (Figure 2), the loops, triradii and whorls of fingerprints, on the fracture behavior of the matrix material. A background discussion of disclinations is presented in the next section, followed by presentation of the research results for this year.

BACKGROUND

The carbonaceous mesophase is a unique liquid crystal formed during the pyrolysis of those organic materials that yield graphitizable cokes or chars^{1,2}. In the temperature range of 400° to 500°C, polymerization reactions occur to build large, disklike, polynuclear aromatic molecules, that, upon reaching molecular weights in the neighborhood of 1,400, condense in parallel arrays and precipitate from the molten pitch as a liquid crystal, the carbonaceous mesophase. Initially, this mesophase forms as small spherules of simple structure, but, after coalescence to viscous bulk mesophase, quite complex morphologies are developed and eventually frozen-in as the pyrolyzing mass hardens to a coke. The carbonaceous mesophase has the structural characteristics of a discotic nematic liquid crystal -- an array of disklike molecules that tend to lie parallel to each other and display long-range orientational order, but are not required to be in point-to-point registry to adjacent molecules³. This liquid crystal is shown schematically in Figure 1. Several possible molecular models are shown, based on the analysis of the mesophase by infrared spectroscopy, nuclear magnetic resonance spectroscopy and vapor pressure osmometry⁴.

In the liquid crystal stage of pyrolysis, the basic morphologies of graphitic materials are established through spherule coalescence and deformation of the mesophase. These complex lamelliform morphologies necessarily contain structural discontinuities, that is, disclinations, in the

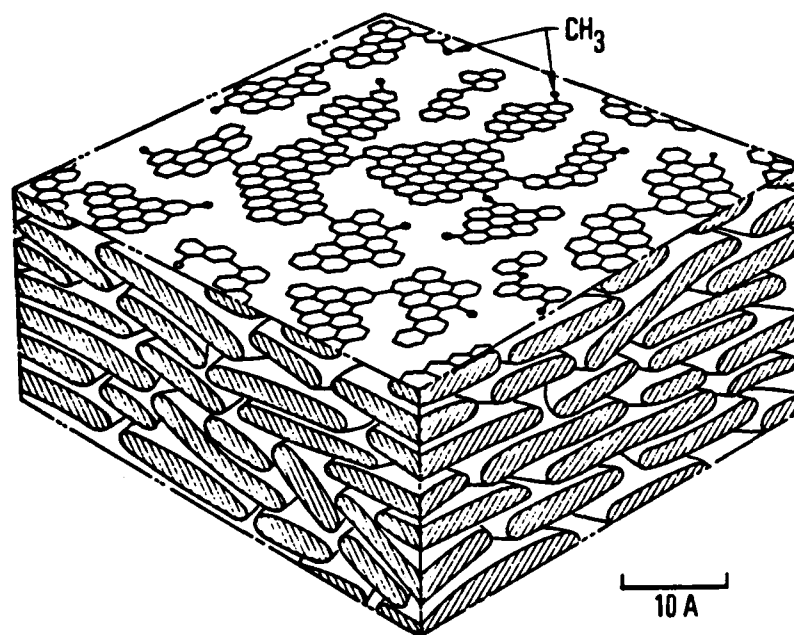


Figure 1. Schematic model of the carbonaceous mesophase, a discotic nematic liquid crystal

parallel stacking of the aromatic molecules⁵. On a local scale, the parallel stacking in the mesophase is retained throughout a region of material. However, the orientation of the stacking changes continuously as the molecule layers bend, splay and twist, and map out singly and doubly curved surfaces. Topologically, space cannot be filled completely by these curved regions of stacked molecules and thus disclinations exist as the discontinuities in this complex morphology. The disclinations are characterized by a rotation vector of multiples of π , as described by the two-fold symmetry of the discotic nematic liquid crystal. For the wedge disclinations of Figure 2, the rotation vector is parallel to the tangent to the disclination line (core), and for the twist disclinations of Figure 3, the rotation vector is perpendicular to the tangent.

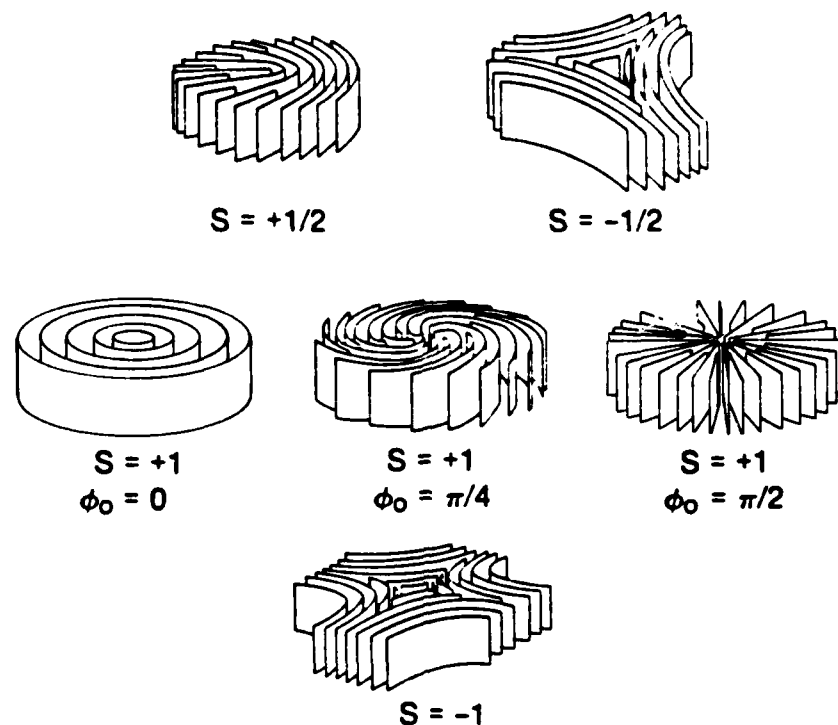


Figure 2. Wedge disclinations in the carbonaceous mesophase. The surfaces denote the layers mapped out by the average direction of the preferred orientation of the individual disklike molecules. The rotation vector is parallel to the tangent to the disclination line.

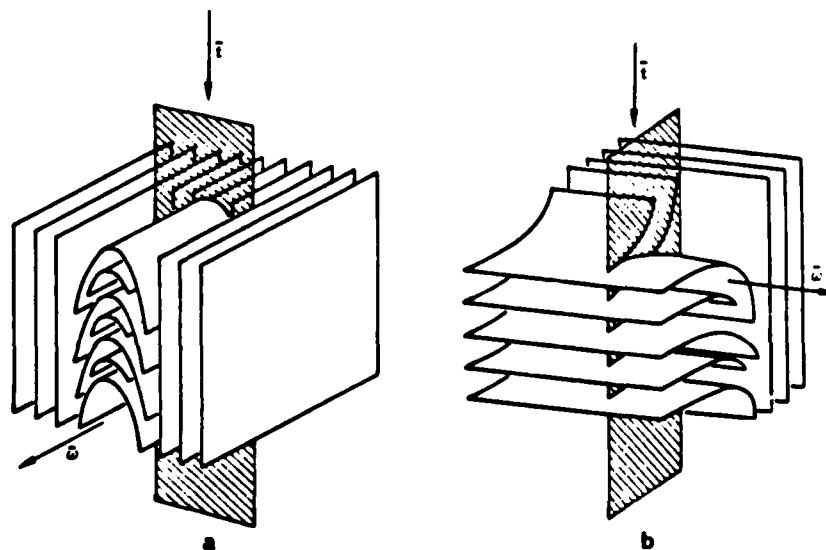


Figure 3. Twist disclinations in the carbonaceous mesophase. The rotation vector is perpendicular to the ribbonlike core.

The disclinations are classified by the amount of rotation involved and its direction relative to the tangent to the disclination line. The strength of a disclination is a measure of this rotation and is determined by considering the change in the direction of the normals to the disklike molecules about a circuit that encloses the disclination line. The change in local orientation of the normals along the closed curve, a Nabarro circuit⁶, is observed. The disclination strength is then defined as the number of revolutions of the direction of the normals with respect to one revolution (2π) about the Nabarro circuit. A Nabarro circuit is illustrated in Figure 4

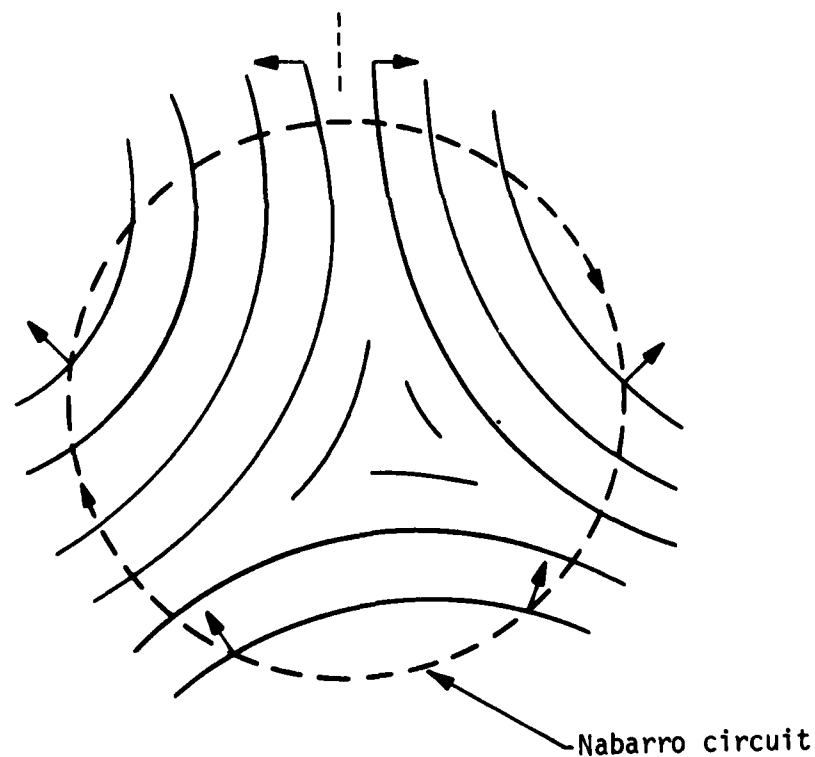


Figure 4. A Nabarro circuit about a wedge disclination. The rotation of the normals is $-\pi$; the strength $S = -\pi/2\pi = -1/2$.

for a negative wedge disclination of rotation π , that is, a wedge disclination of strength $S = -1/2$. The amount of the rotation of the normals is π , and the rotation is counter (negative) to the direction of the Nabarro circuit.

The crystal defects known as disclinations were conceived many years ago by theoreticians as a part of the general pattern of possible distortions in crystal lattices⁷. Owing to the high lattice distortions involved in these rotational distortions, it was considered unlikely that disclinations would play a significant role in any structural material. However, disclinations were subsequently found to be prominent features of liquid crystals in which the point-to-point lattice registry between adjacent molecules is not required, thus greatly relaxing the strain fields around the disclination cores. Since the morphologies of carbon-carbon composites are established while the carbonaceous material is in the liquid-crystalline state, the presence of disclinations in these lamelliform morphologies is to be expected. The existence of these layer-stacking defects was demonstrated in 1967⁸, and evidence of wedge and twist disclinations has subsequently accumulated^{9,10}.

The presence and types of disclinations is efficiently determined by reflection microscopy with polarized light. The preferred orientation of the mesophase as it intersects a polished plane of section can be defined with cross-polarized light. Crystalline graphite is birefringent (optically anisotropic) and thus the reflection of polarized light is dependent on its orientation to the preferred orientation of the mesophase. The reflection contrasts for a graphite single crystal are illustrated in Figure 5. With polarized-light micrography, disclinations are evident as rotation-invariant points in the extinction contours that identify mesophase layers that are perpendicular to a polarizing direction. The disclinations of strength $\pm 1/2$ are denoted by a node with two extinction-contour arms. For a rotation of the

crossed polarizers, the arms of the $S = +1/2$ node rotate with the polarizers and the arms of the $S = -1/2$ node rotate counter to the polarizers. The disclinations of strength $S = \pm 1$ are denoted by a cross in the extinction contours -- a point with four extinction-contour arms. The $S = +1$ disclination is a corotating cross; the $S = -1$ disclination is a counterrotating cross. The polarized-light micrography at various angles of rotation of the polarizers is used to define the molecular orientations about these nodes and crosses in the extinction contours and thus map out the configurations of the underlying disclinations².

The identification of the disclinations in the carbonaceous mesophase has been aided by the use of mesophase microconstituents that have a strong preferred orientation. The two microconstituents are the fibrous and lamellar constituents which result from uniaxial and biaxial extension, respectively, of the plastic mesophase. The microconstituents are the needle-like portions of the needle coke and the lamellar bubble walls of voids in the mesophase.

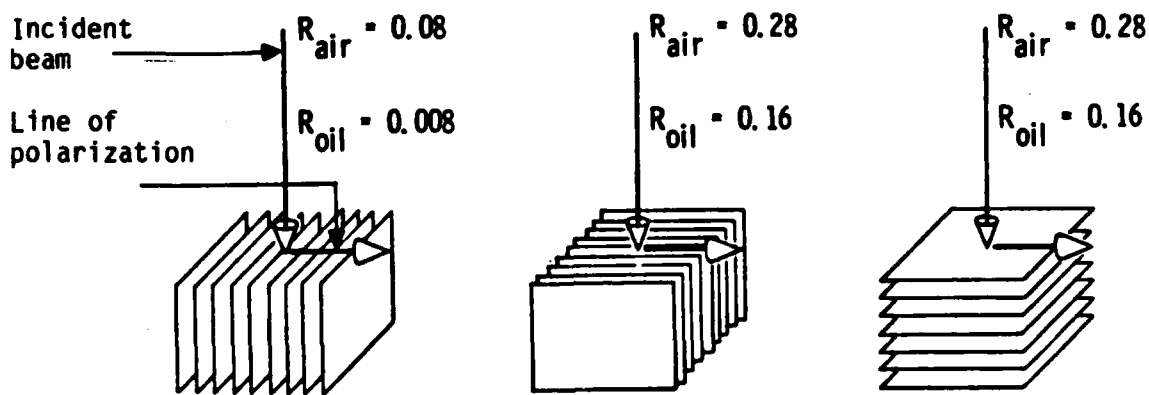


Figure 5. Reflectance of polarized light from a graphite crystal. The differences in reflectance for the carbonaceous mesophase are slightly smaller, but significant to delineate the disclination structures.

These microconstituents have offered good subjects for detailed study because the strong preferred orientation of each microstructure relative to selected planes of section provided the information necessary for resolution of the disclination structures. However, the mesophase which fills the matrix pockets of a multidirectional graphite-fiber preform may not have a distinct preferred orientation, and the array of wedge and twist disclinations may be quite complex.

Another advantage of the carbonaceous mesophase for the study of disclinations is that the mesophase can be quenched to a solid which can be sectioned and studied by optical micrography. Perpendicular planes of section and successive parallel planes of section are used to define the mesophase morphology in three dimensions¹¹.

Carbon-carbon composites are leading candidate materials for applications that require retention of mechanical properties at high temperature, good thermal-shock resistance, and resistance to chemical erosion. The carbonaceous mesophase plays a key role in the fabrication of these composites, and thus these properties are dependent on the mesophase morphology formed in each constituent of a carbon-carbon composite. The processing procedures directly control the microstructure of the matrix of the carbon-carbon composites. Densification of these composites involves impregnation with an organic precursor, carbonization and graphitization. Variations include the type of precursor (petroleum pitch, coal-tar pitch, or thermosetting resin), the applied pressure during carbonization, and the graphitization temperature.

The complex, heterogeneous structure of the multidirectional carbon-carbon composites consists of fiber bundles and matrix pockets, each with their own distinct microstructures. Disclinations exist in the matrix within

the graphite-fiber bundles and in the matrix regions between fiber bundles. Each has its characteristic disclination structure and thus may play a different role in the relation of disclinations to the properties of the carbon-carbon composites.

THREE-DIMENSIONAL ARRAYS

In a typical volume element of the carbonaceous mesophase, the disclination lines are oriented in many different directions. The lines may be curved or straight, and they may intersect each other. Identification and characterization of such a complex, three-dimensional array of disclinations is not simple. Although much information can be obtained from optical and scanning electron microscopy of a single metallographic plane of section, this analysis provides no information on the disclination arrays normal to this plane in the third direction. One technique to characterize the three-dimensional structure of the disclination arrays is to use mesophase microstructures with a high degree of preferred orientation⁵. These include the fine fibrous structure of needle coke, the lamellar structure of bubble walls, and the aligned matrix in a graphite-fiber bundle. However, these specific microstructures are not always present in a carbon-carbon composite, especially in regions of the matrix between fiber bundles. Thus, another technique is needed to characterize the disclination arrays in matrix material that does not have a preferred orientation. This technique involves observation of a specific area on successive parallel planes of section.

In the first annual report¹², some features of the disclination arrays were identified. These features are those that are observed on a single plane of section. There tends to be an equal number of positive and negative disclinations such that the net rotation (strength) of a region of mesophase

tends to zero. Disclinations of strength $S = \pm 1/2$ are more prominent than disclinations of strength $S = \pm 1$, since the energy of a disclination is related to the square of its strength. And along an extinction contour line, the disclinations alternate sign.

The observation of the three-dimensional arrays of disclinations was designed to determine whether the disclination lines are straight or curved, at what angles they intersect a typical single plane of section, and whether the disclinations intersect, and in what manner they intersect.

Experimental Procedure

The technique of observing the same area on successive parallel planes of section required precise thickness measurements, skillful polishing, and careful procedures. Although tedious, this technique provided the information sought. The sample used was carbonaceous mesophase from Ashland A240 petroleum pitch heat treated at 400°C for 24 hr. This heat treatment produced mesophase with a coarse, undeformed microstructure with no specific preferred orientation. This mesophase microstructure is typical of the large matrix regions between fiber bundles in a carbon-carbon composite. The sample was mounted in epoxy and polished, ending with a final polish with 0.05 μm cerium oxide powder. For referencing the sample to the exact same location after each polishing, a special right-angle centering device was mounted firmly on the microscope stage. The Neophot 21 (Zeiss aus Jena) reflected-light microscope has an inverted stage for easy access. To obtain planes of section below the previous plane of section, the sample was polished with the final polish until the desired thickness of material was removed. Thickness of the sample was measured with a tooling micrometer with an accuracy of $\pm 1.3 \mu\text{m}$ (0.00005 inch). Three points about the sample were measured to ensure parallelism. Optical micrographs were taken after each plane of section of the same referenced area, as indicated in Figure 6.

To encompass an area of the mesophase sample which had a reasonable number of disclinations which could easily be identified, a magnification of 800 was chosen. The area observed then on the micrograph was about 110 by 130 μm . Since the spacing between disclinations on the first plane of section was about 10 to 20 μm , the distance between the planes of section needed to be slightly less than this spacing. A spacing of 5 to 10 μm was chosen to provide a fine enough scale to observe any subtle changes in the location of the disclination lines. Eight planes of section were observed; the total depth was 46 μm .

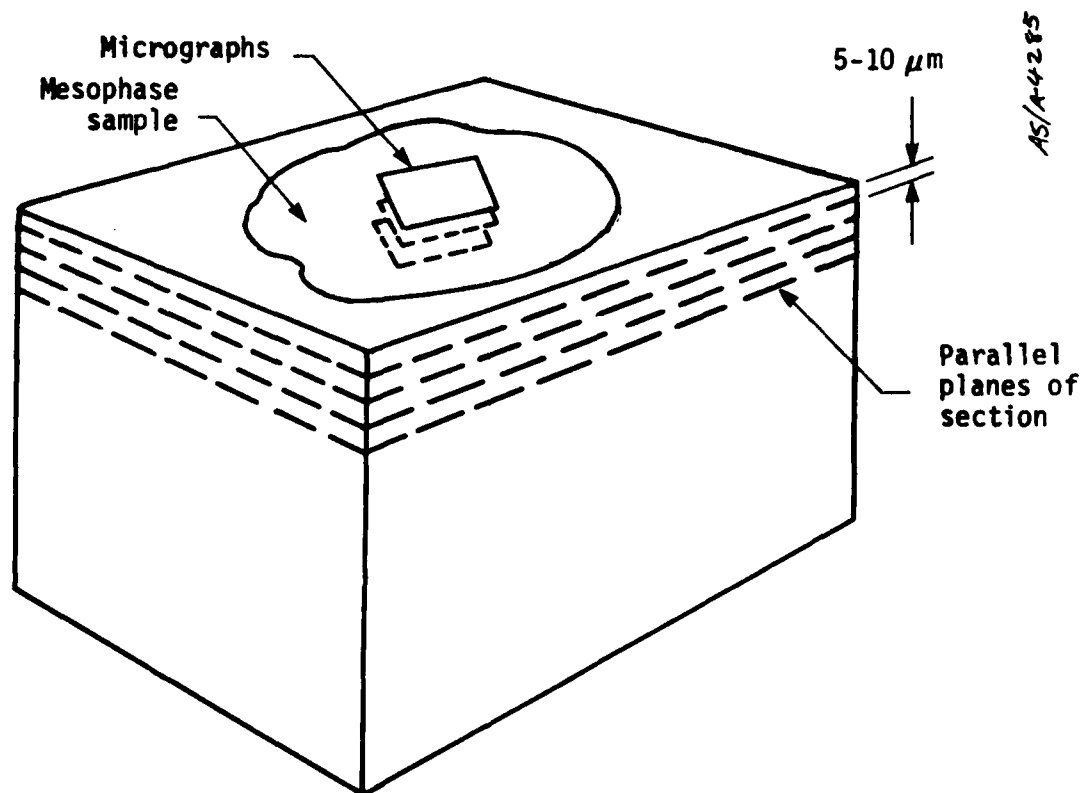


Figure 6. Schematic diagram of micrographic technique for observing three-dimensional disclination arrays

For each micrograph for each plane of section, a structural sketch was made to identify the underlying mesophase microstructure, including the disclinations. A series of micrographs at various rotations of the crossed polarizers were made and, with the use of an overlay, the orientation of the layers in the mesophase was sketched at each rotation. These structural sketches were then used to construct a three-dimensional picture of the disclination array. The core of each disclination was plotted, and the points connected to define the path of the disclination lines in-depth in the sample below the original plane of section. Eventhough great care was taken to prevent any shift in the position of the sample prior to taking each micrograph, there was some shift (less than $2\ \mu\text{m}$) in the position of the sample due to slight temperature fluctuations. Thus, in preparing the three-dimensional model of the disclination array, the corner of the micrographs was not used to align the set of micrographs. Instead, one disclination that appeared to be rather straight and normal to the planes of section was used as the reference for the alignment of the micrographs.

Results

The optical micrographs of the same area of mesophase on eight successive parallel planes of section are shown in Figures 7 through 14. With each micrograph is the structural sketch of the disclination structures. As evident in Figure 7, the original plane of section, is one extinction-contour cross ($S = +1$ disclination) and several extinction-contour nodes ($S = \pm 1/2$ disclinations). This set of micrographs show that there is some change in the disclination array. Some of the change is difficult to identify; some of the change is slight and can be easily recognized. For example, the three $S = 1/2$ disclinations in the lower right-hand corner maintain their position through the seven planes of section. Over the distance of the eight planes of

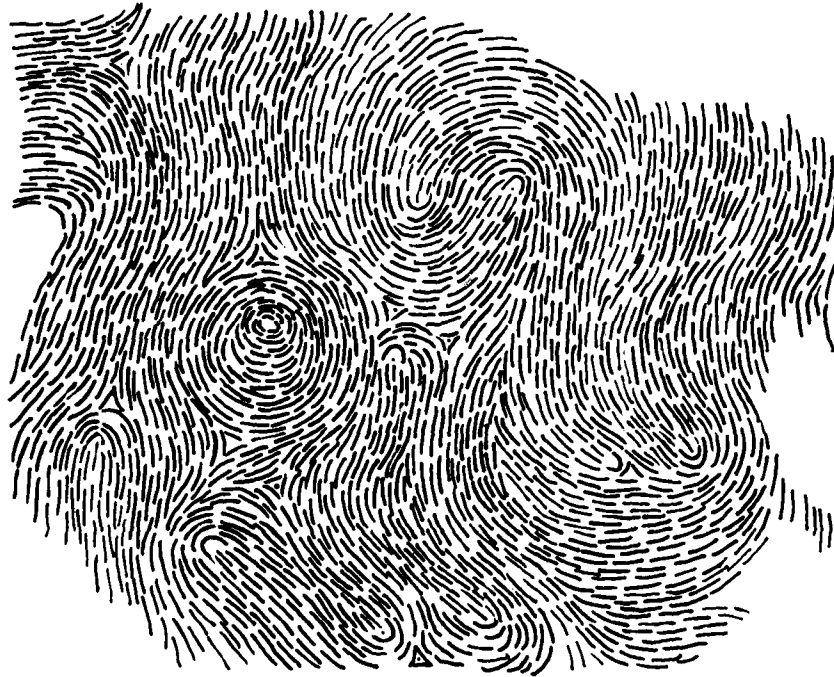


Figure 7. Optical micrograph and structural sketch of disclination array in carbonaceous mesophase; first plane of section, cross-polarized light

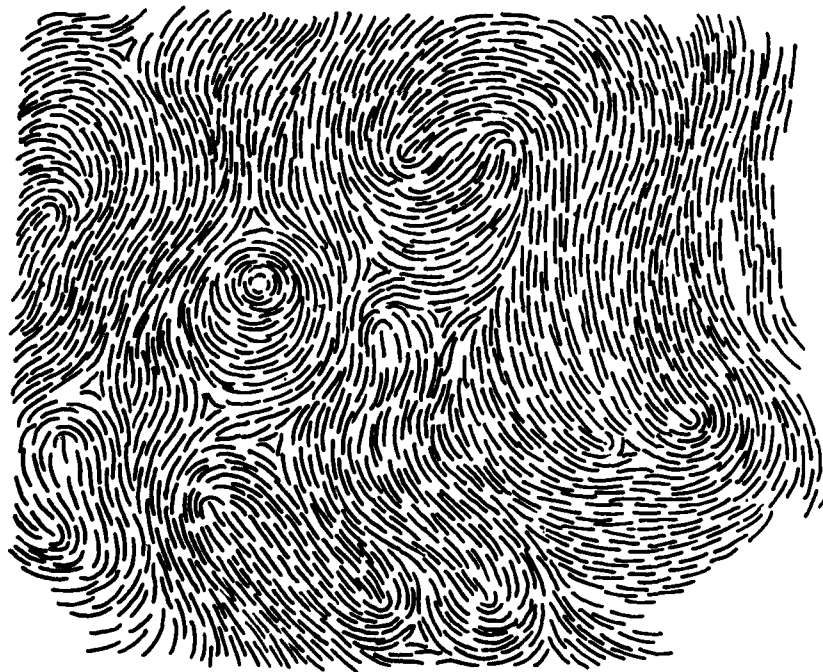
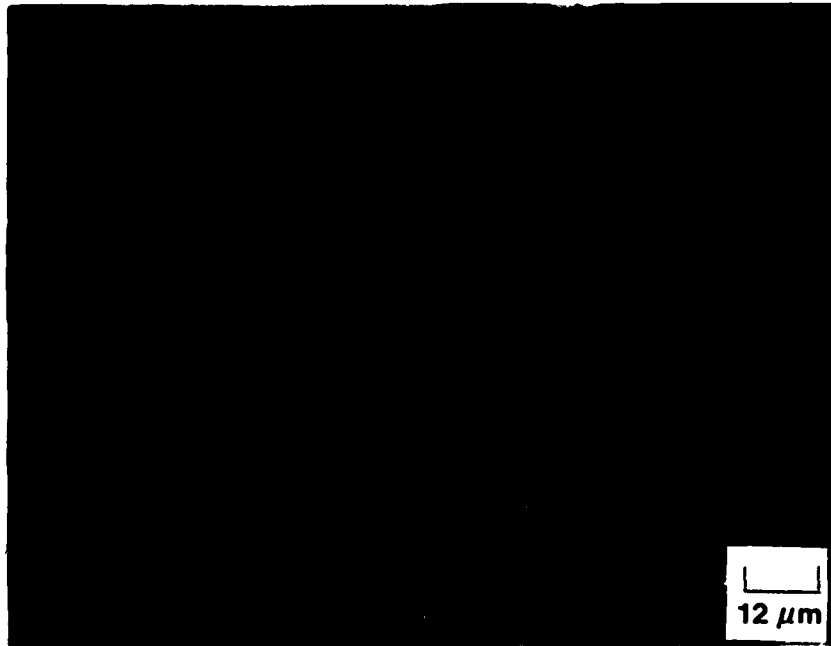


Figure 8. Optical micrograph and structural sketch of same area as Figure 7 on second plane of section $5\ \mu\text{m}$ below first plane

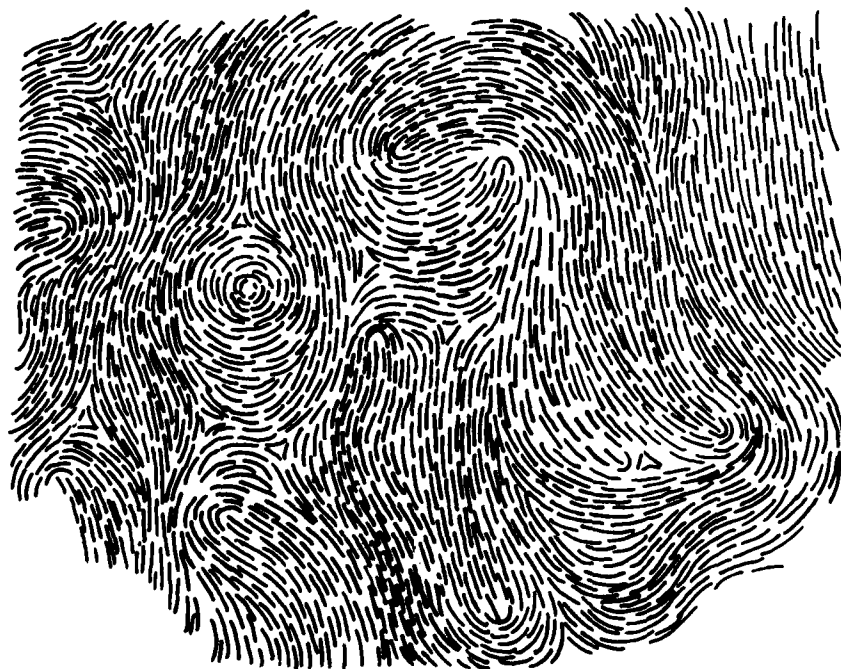
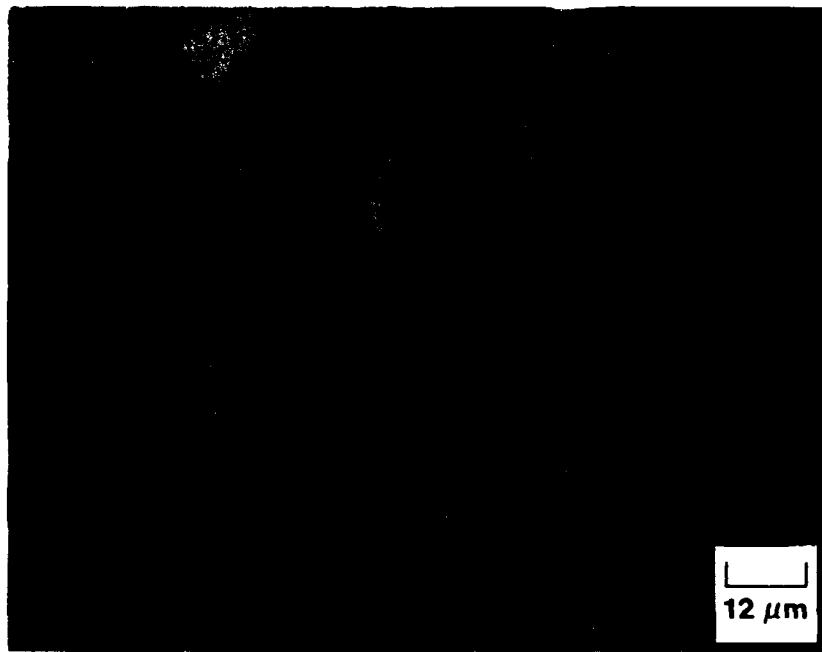


Figure 9. Optical micrograph and structural sketch on third plane of section, 10 μm below second plane



H-213

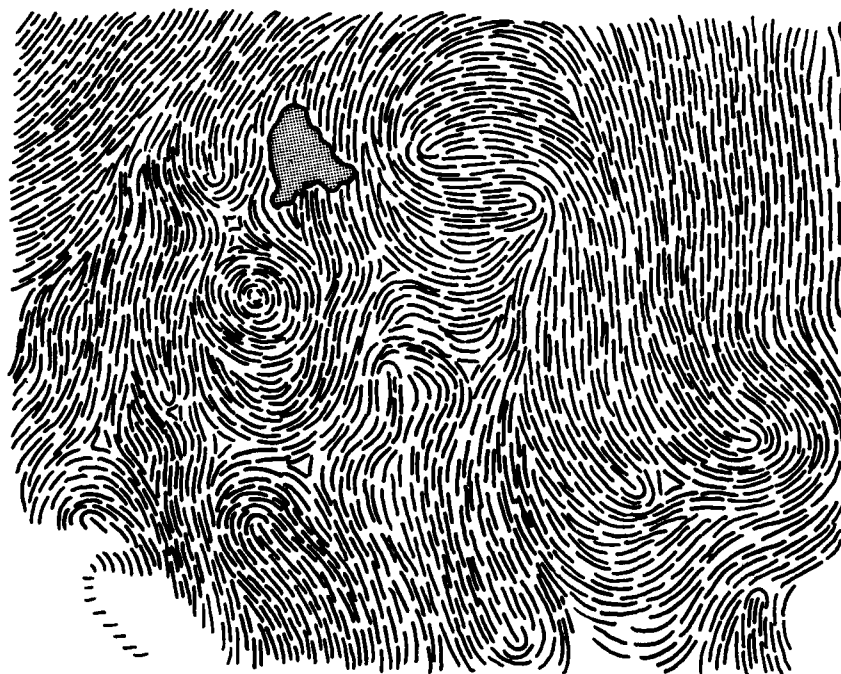


Figure 10. Optical micrograph and structural sketch on fourth plane of section, 8 μm below third plane



H-212

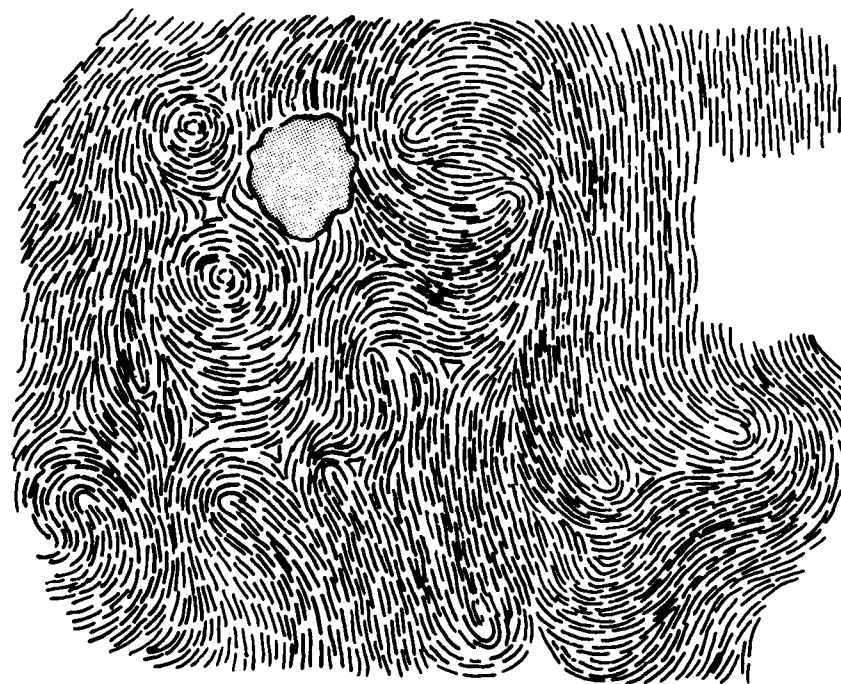


Figure 11. Optical micrograph and structural sketch on fifth plane of section, 5 μm below fourth plane

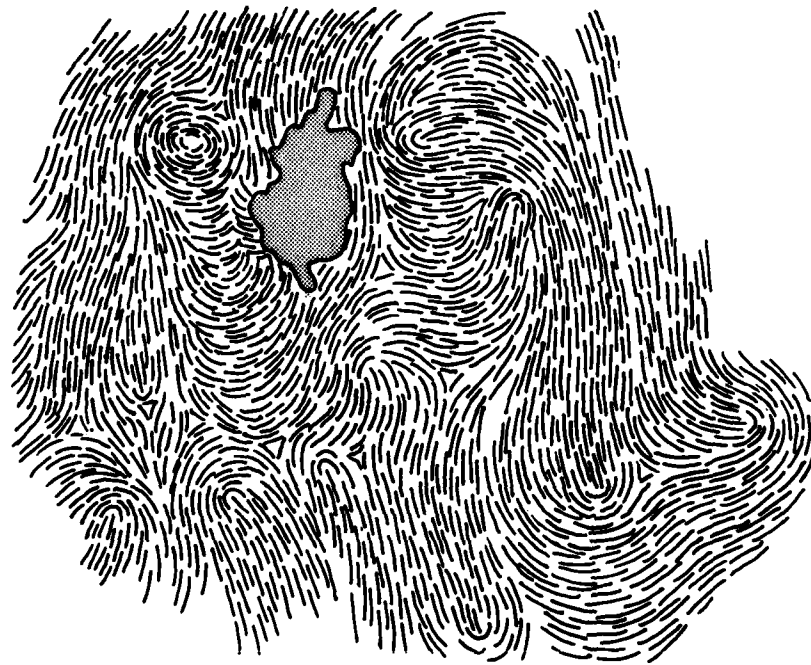
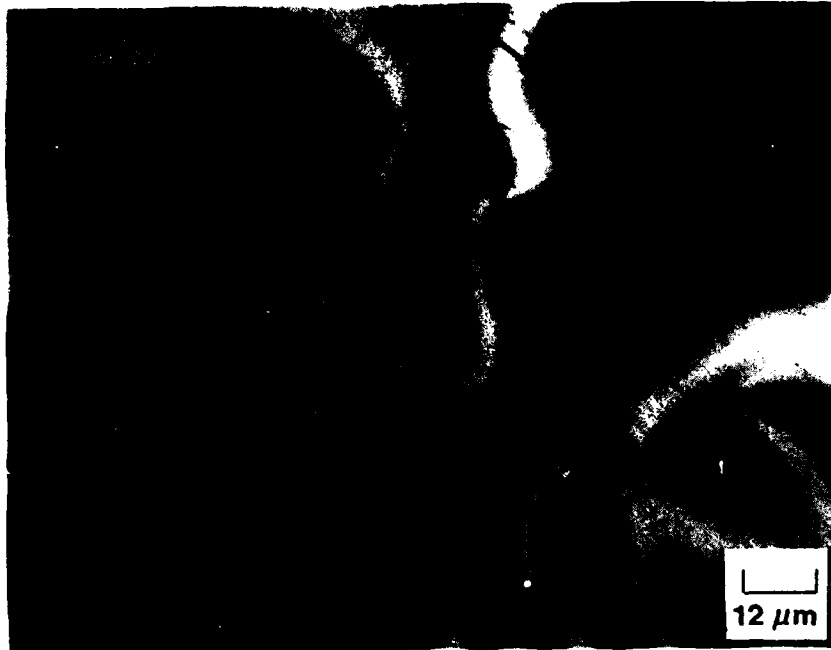


Figure 12. Optical micrograph and structural sketch on sixth plane of section, 5 μm below fifth plane

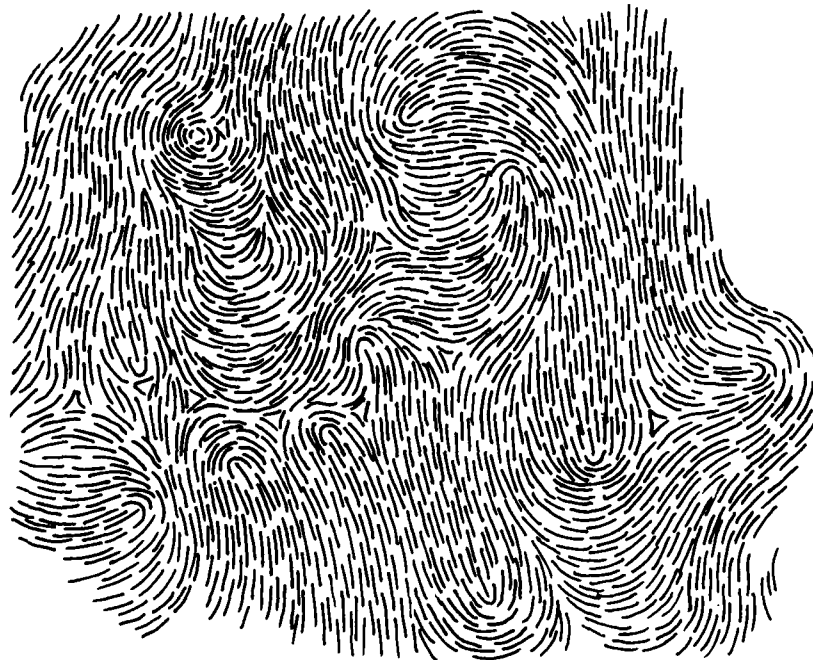


Figure 13. Optical micrograph and structural sketch on seventh plane of section, 8 μm below sixth plane



H-237

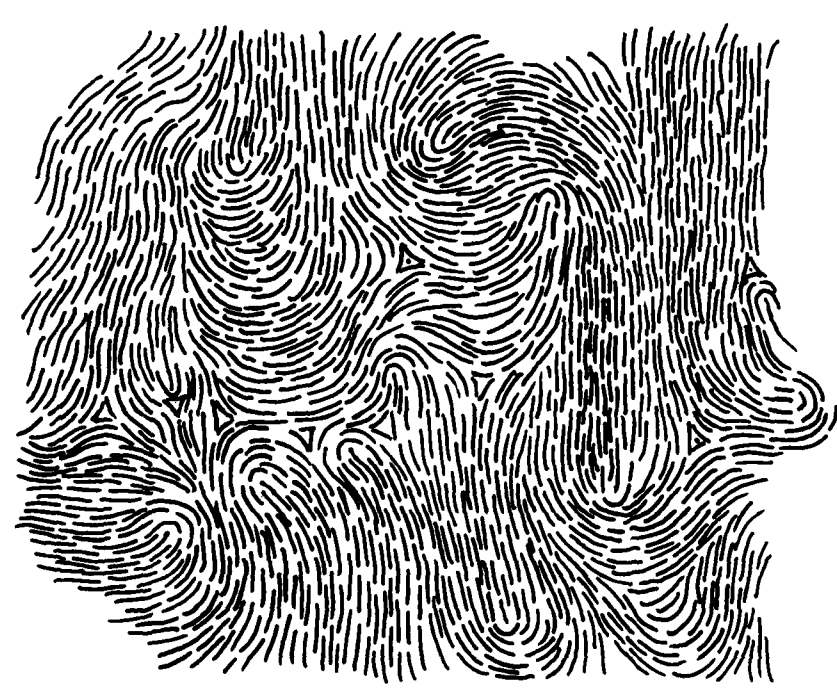


Figure 14. Optical micrograph and structural sketch on eighth plane of section, 5 μm below seventh plane

section, none of the disclinations end abruptly. Topologically, a disclination line cannot end in the material. However, if the disclination were a point disclination, it would appear to end (vanish) on a subsequent plane of section. Thus, all the disclinations are line disclinations. Also, since their position on each successive micrograph changes, they intersected the original plane of section at angles other than 90° .

A three-dimensional sketch of the disclination array is presented in Figure 15. The points of intersection of each disclination line with each plane of section have been connected to illustrate the path of each disclination line. The lines generally traverse from the front face of the volume of mesophase to the back face (last plane of section). Each type of disclination is represented by a different type of line. The apparent axial symmetry of these disclinations suggests that these disclinations are wedge disclinations.

Even though this mesophase sample appeared to have a coarse, undeformed microstructure, and the area photographed was chosen arbitrarily, there is some preferred orientation of this disclination array. The disclination lines are relatively parallel. In the coarse microstructure, the disclination array might be expected to appear more like a tangled ball of string. Apparently, in the small volume observed here, there is a slight preferred orientation. On a larger scale, the structure is more isotropic. Observation of the smaller volume (at high magnification) was necessary to distinguish between the disclinations.

Two significant features of the disclination array are evident. First, the disclination lines are curved. Over this small distance between the eight planes of section ($46 \mu\text{m}$), the amount of curvature is not great. The disclination on the lower right-hand corner is straight, as it is the

- $S = -1/2$
- $S = +1/2$
- $S = +1$
- .-.-.- $S = -1$

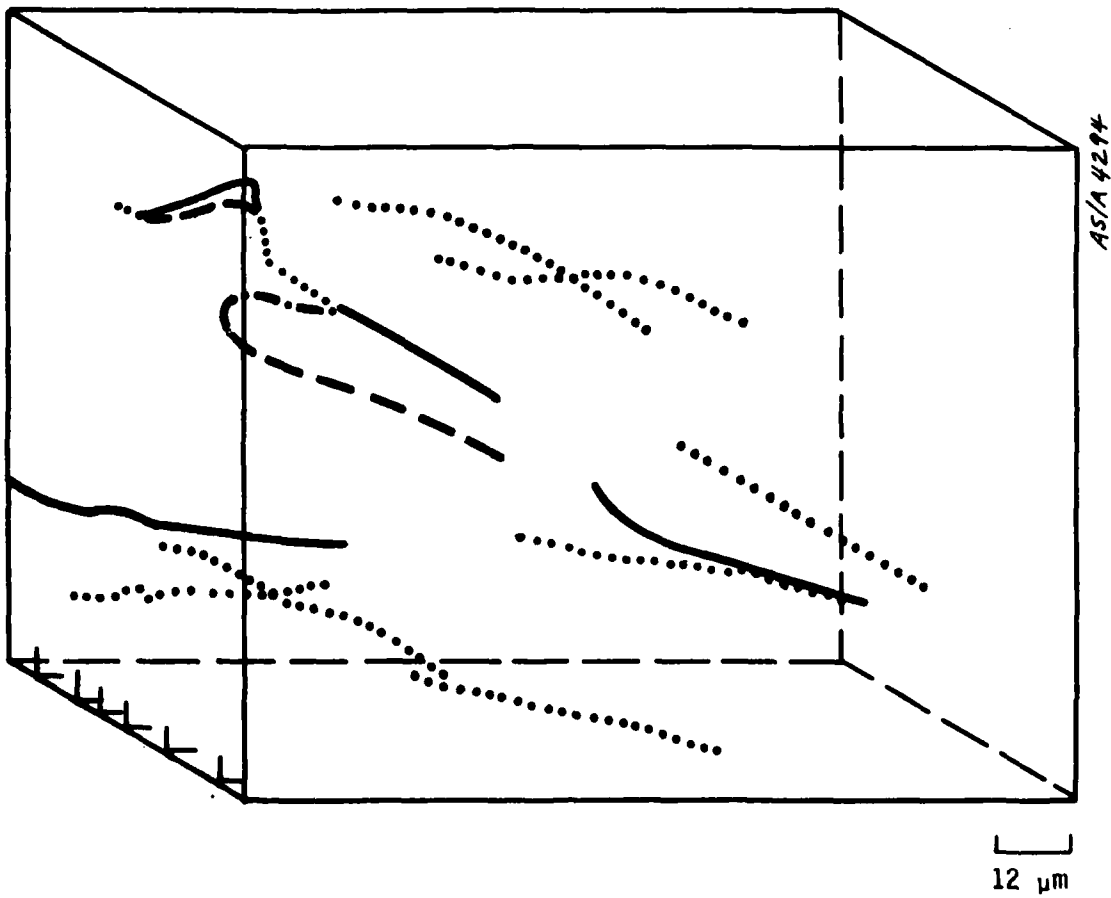


Figure 15. Sketch of the three-dimensional structure of the disclination array. The disclination lines begin on the front face (first plane of section) and end on the back face (eighth plane of section).

reference disclination. For any plane of section, the disclinations are not generally normal to that plane.

Second, and more interesting, is the evidence for the interaction of the disclinations. One disclination can separate into two disclinations, and two disclinations can join to one. The strength of such an interaction is conserved, that is, the total strength before the interaction equals the total strength after the interaction. For example, the first interaction consists of an $S = -1/2$ disclination branching to an $S = +1/2$, and an $S = -1$ disclination: $(S = -1/2) \rightarrow (S = +1/2) + (S = -1)$, or $-1/2 = +1/2 - 1$. In some cases, the disclination lines cross only due to the perspective view. In actuality, they do not cross, but their positions change or rotate, giving the appearance of the crossing of the lines. This group of disclination interactions is sketched in Figure 16, as projected on a vertical plane normal to the planes of section. Each interaction is identified. The disclination structures on the planes of section on both sides of the disclination interactions are sketched in Figure 17. Between the planes of section, the layer structure changed from the structure in one sketch to the structure in the other sketch. The details of this change can be inferred from these pairs of sketches, but the three-dimensional structure is both difficult to visualize and to sketch.

This is the first evidence for these disclination interactions in solid carbonaceous mesophase. This evidence was possible only by the technique of successive parallel planes of section. Similar disclination reactions have been observed by hot-stage microscopy on the free surface of the mesophase as a liquid^{13,5}. In this case, the disclinations interacted due to viscous flow of the mesophase, but the interactions were observed only on this single

45/A 4925

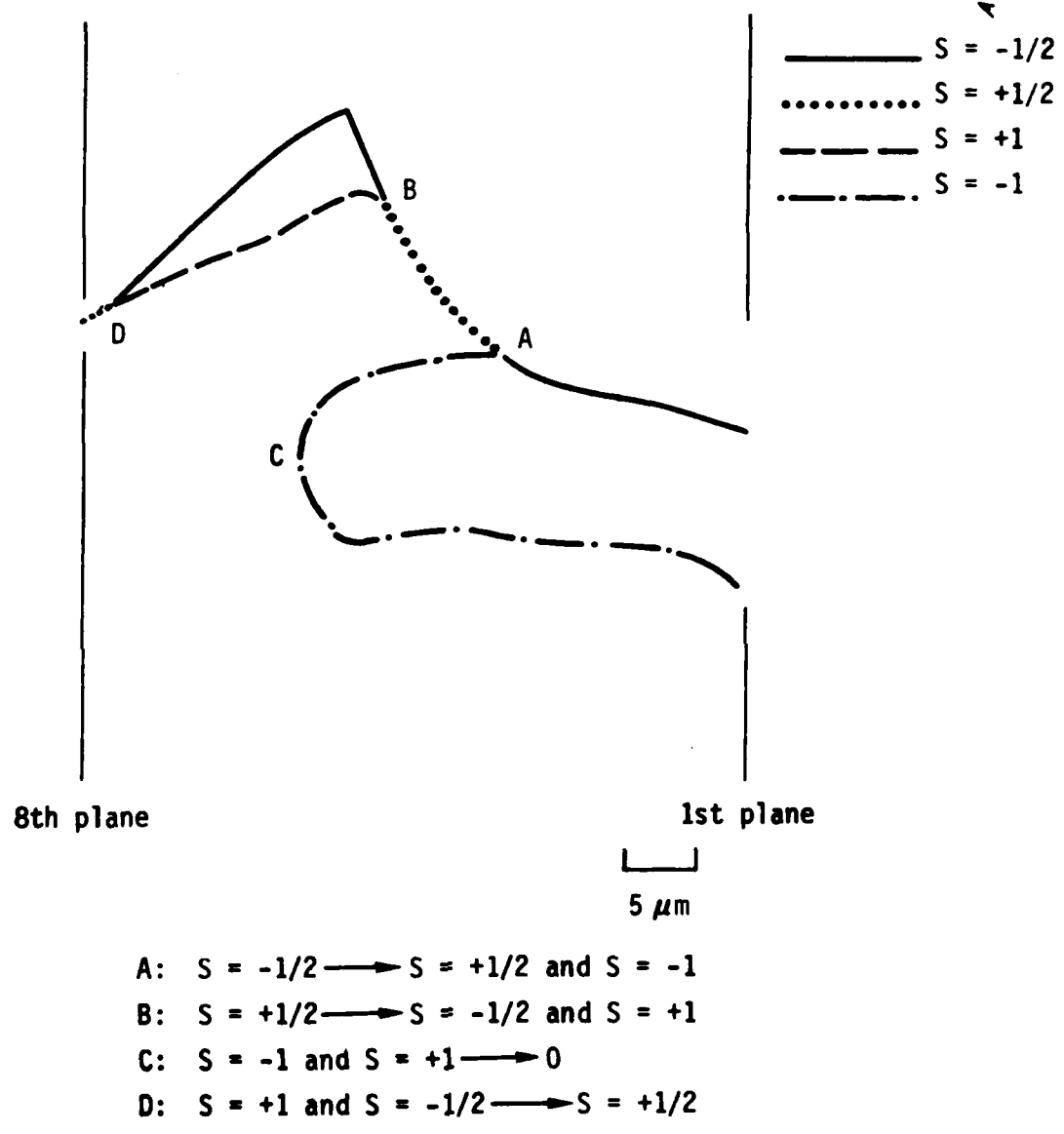


Figure 16. Projection of disclination array containing interactions on vertical plane normal to planes of section. The strength of each interaction is conserved.

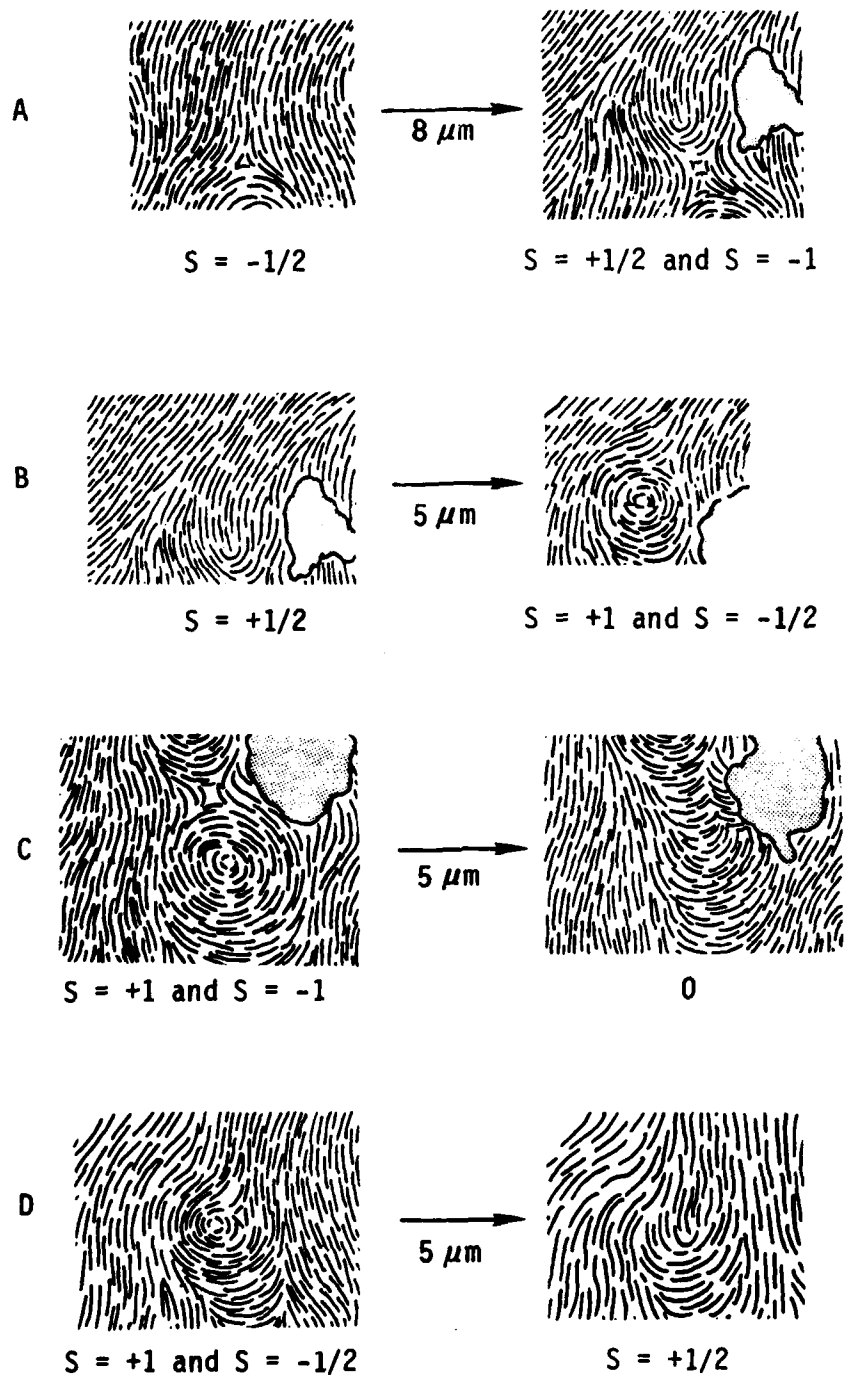


Figure 17. Sketches of disclination interactions on adjacent parallel planes of section

surface. The nature of the disclination arrays and reactions in-depth could not be observed.

This evidence of the disclination interactions indicates the complexity of an array of disclinations. Although much information can be obtained from a single plane of section through the carbonaceous mesophase, the complex, three-dimensional network of disclinations is hidden below this single plane of section. This complex network of disclinations probably provides a difficult fracture path for the matrix of a carbon-carbon composite. This type of fracturing was documented in the first annual report¹². For matrix with more preferred orientation, as in a fiber bundle, such fracturing may be easier to identify. This type of fracturing is discussed in the next section.

SHEAR FRACTURE AND DISCLINATIONS IN A CARBON-CARBON COMPOSITE

The basic relation of disclinations to the fracture of the carbonaceous mesophase was identified in the first annual report¹². Crack paths in the mesophase coke were observed with cross-polarized-light micrography, which indicated in a qualitative way that the disclinations present in the microstructure of these graphitic materials contribute to crack blunting and crack diverting. This absorption of fracture energy results in a high work of fracture for graphitic materials formed via the carbonaceous mesophase.

Disclinations are abundant in carbon-carbon composites fabricated with matrices from petroleum or coal-tar pitch. The fracture behavior of these composites can thus be expected to also be influenced by the disclinations present. This present work has investigated the qualitative effect of disclinations on shear-type cracks in a carbon-carbon composite. The composite used was a two-directional composite fabricated with graphite-fiber fabric of Hercules HM 1000 polyacrylonitrile filaments woven in an eight-harness-satin weave. The fabric laminate was densified with Allied 15V coal-tar pitch by carbonization at 103 MPa and graphitization at 2700°C. The final bulk density was 1.95 g/cc. Specimens of this composite, oriented parallel to each fiber direction, were tested in short-beam shear at a span-to-depth ratio of 4:1. The plane containing the length and thickness directions was polished, and the interior shear-induced cracks were observed with both optical and scanning-electron microscopy. For the electron micrography, the samples were

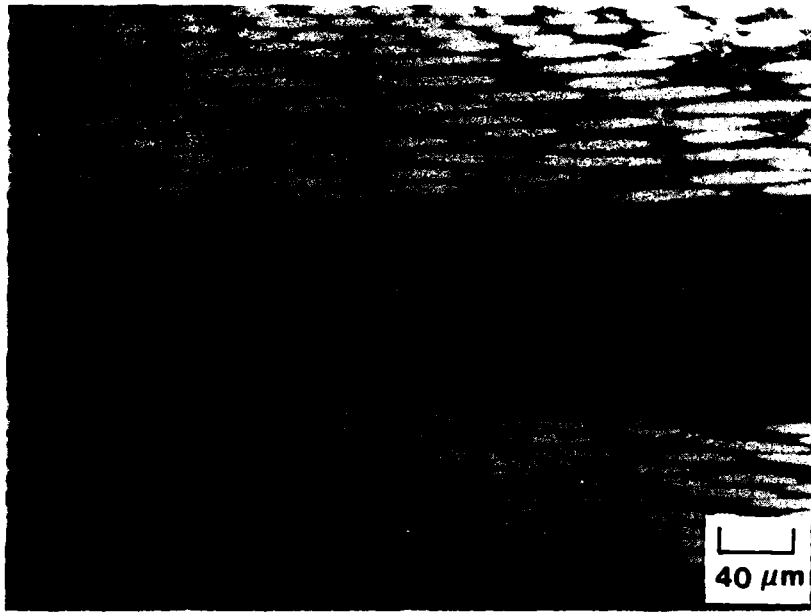
ion etched with zenon to produce a surface relief that denoted the orientation of the underlying graphitic structure^{5,11}.

Optical Micrography of Shear Cracks

The basic construction of the two-directional composite is shown in Figure 18. The two principal fiber directions are (nearly) parallel and perpendicular to the plane of section. The shear cracks present extend through the width of the specimen perpendicular to the plane of section. The shear cracks occur in the fiber bundles and at the attachment region between adjacent fiber bundles.

The shear cracking near the perimeter of a fiber bundle is shown in Figure 19. These optical micrographs were taken with bright-field illumination. The response of the graphitized composite to polarized light is not as distinct as the response of the carbonaceous mesophase. Also, the fine cracks are more prominent in the bright-field micrographs. The type and location of disclinations were determined with polarized light before each micrograph was taken. In general, the shear crack tends to follow the graphitic layers which are aligned parallel to the surface of the individual graphite filaments. The shear-crack paths are jagged due to the presence of the disclinations. The most distinct feature of this cracking is the sharp-angle fracturing. This is highlighted by the tongue-and-groove fracturing where a small piece of matrix has been pulled away from the opposite side of the crack. These pieces have distinct angles characteristic of the angles of the graphitic layers of the wedge disclinations of strength $S = -1/2$.

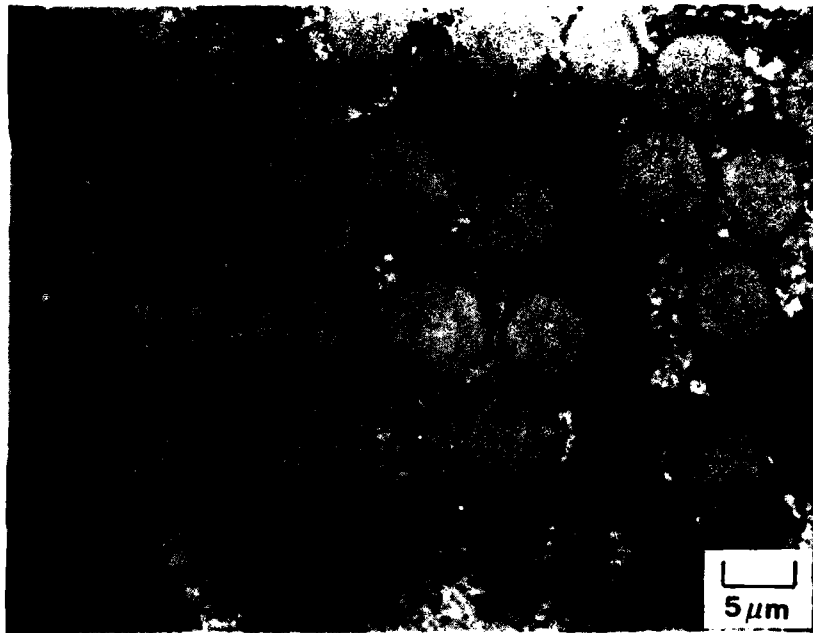
Similar shear fracturing in the fiber bundles (Figure 20) is characterized by the vee-shaped tongues and grooves. Elsewhere the cracks tend to follow the graphitic layers about the filaments. The fracturing also occurs more in the matrix rather than at the fiber-matrix interface. In Figure 21,



H-228



Figure 18. Optical micrographs of shear cracks in two-directional carbon-carbon composite



H-227

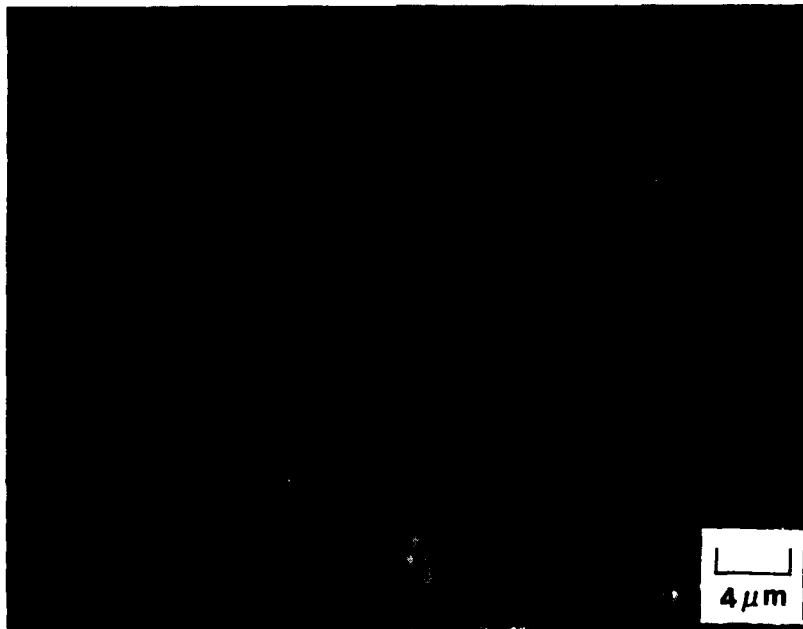
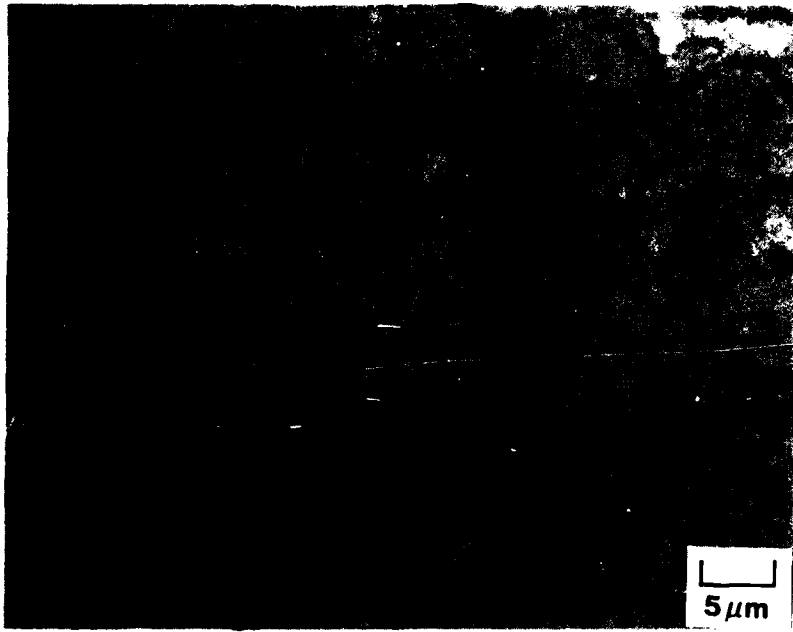


Figure 19. Optical micrographs of shear cracks in fiber bundle near its edge



H-229

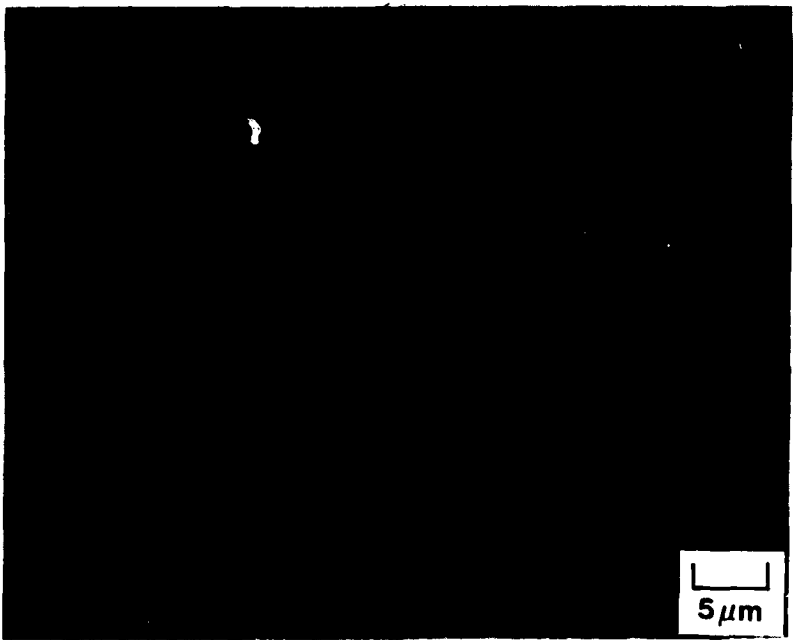
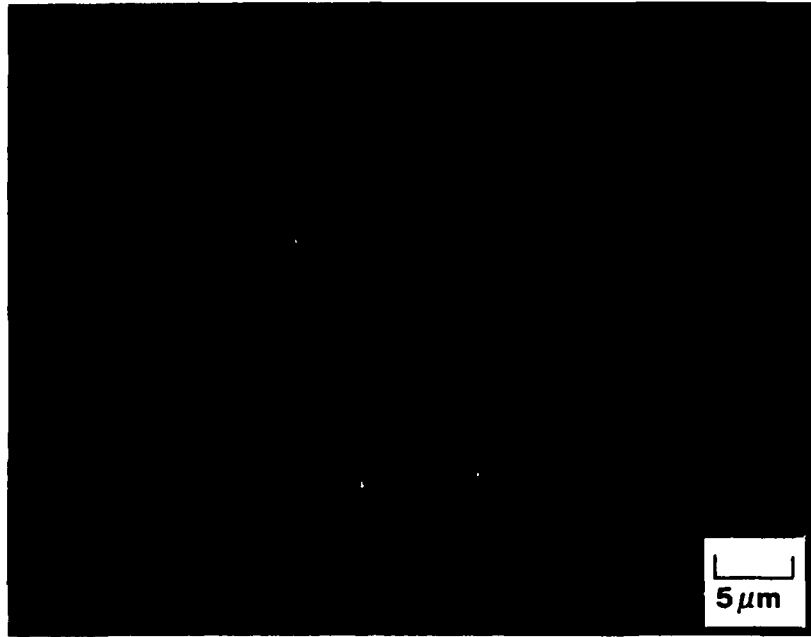


Figure 20. Optical micrographs of shear cracks in fiber bundle



H-207

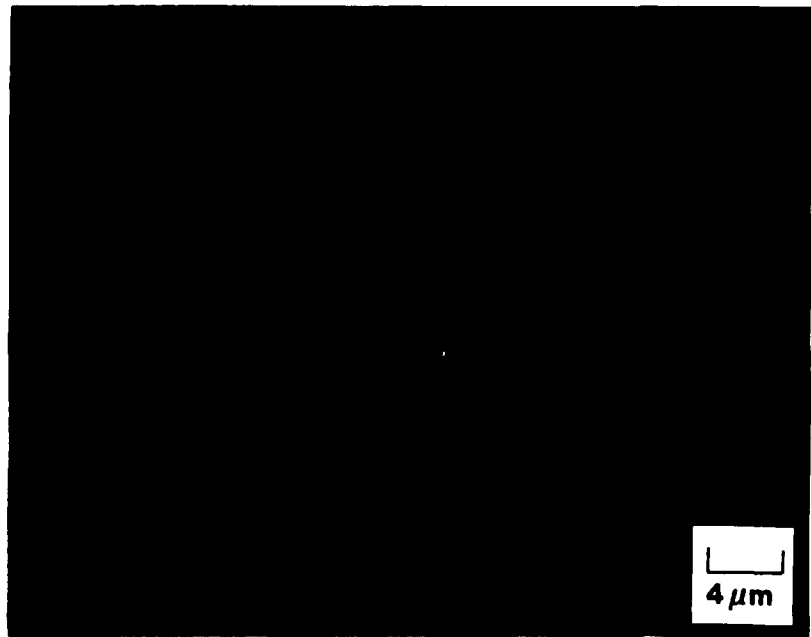


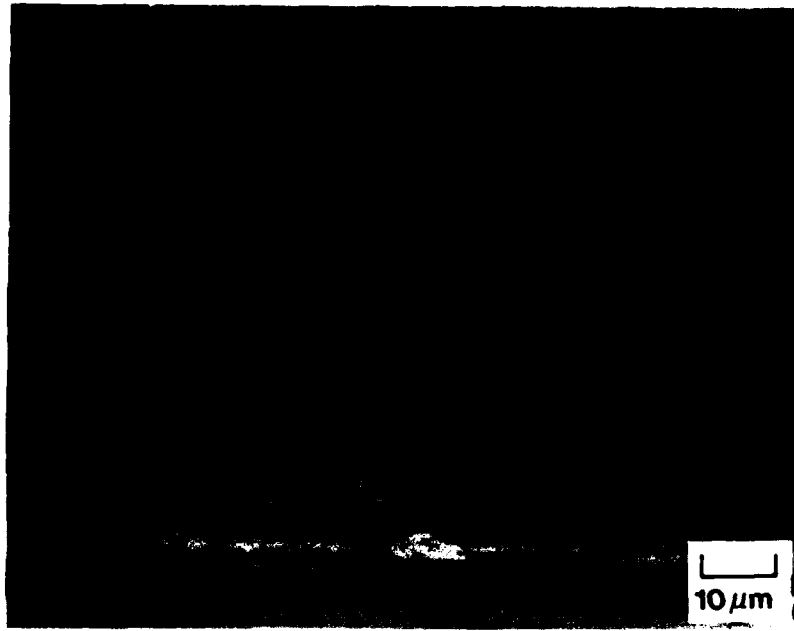
Figure 21. Optical micrographs of shear crack in fiber bundle

fracturing occurred on three sides of a disclination of strength $S = -1$, which is still attached to a filament. Figure 22 shows additional examples of the shear-crack features characteristic of fracturing which is controlled by the disclinations of strength $S = -1/2$ and $S = -1$ present. Near the center of the micrographs of Figure 23 is a crack traversing a disclination of strength $S = -1/2$. Here the separation is not large, and the two halves of the crack indicate the crack diverting and multiple fracturing of the matrix by the disclinations present.

Although these optical micrographs identify the effect of the disclinations on the shear fracturing in the carbon-carbon composite, the optical micrography has a limited resolution. To better define this fracturing and the structure of the disclinations, the shear specimens were observed in a scanning electron microscope. A discussion of these micrographs follows.

Scanning Electron Micrography of Shear Cracks

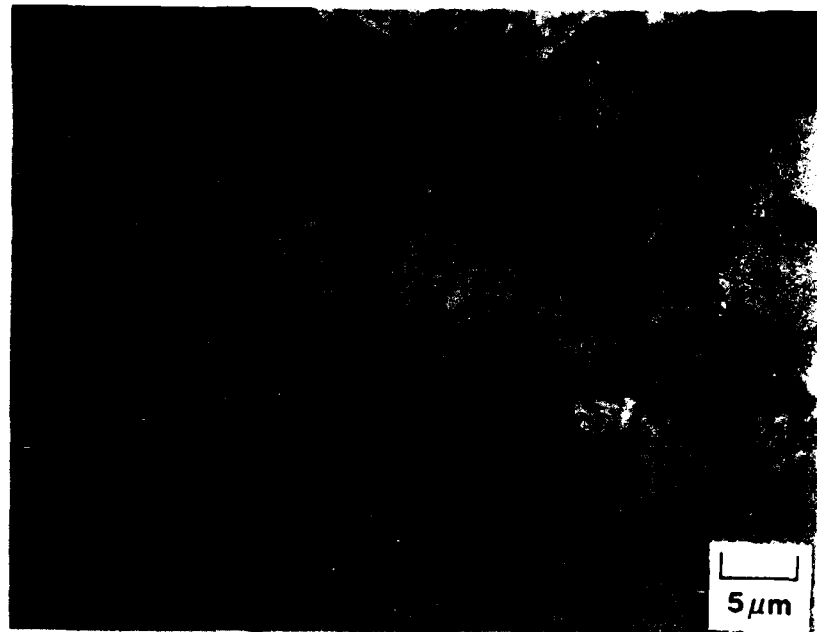
Scanning electron micrographs of a typical shear-induced crack in the short-beam shear specimens of the two-directional carbon-carbon composite are shown in Figure 24. The orientation of the graphite crystallites of the matrix microstructure are easily evident from the ion etching. The alignment of the crystallites in a sheath about each filament is evident. To ensure a flat surface during polishing, these specimens were vacuum impregnated with an epoxy mounting medium. The shear cracks are filled with epoxy, some of which has been removed by the ion etching. Thus, any material in the cracks should be ignored. This figure illustrates the tortuous path of the shear crack in the complex structure of the matrix among the graphite filaments. A segment of this same crack is shown in Figure 25. The tortuous path is highlighted by the regions that have been fractured away from the main crack path in a tongue-and-groove pattern. Cleavage parallel to the orientation of the



H-234



Figure 22. Optical micrographs of shear crack at region between perpendicular fiber bundles



H-220

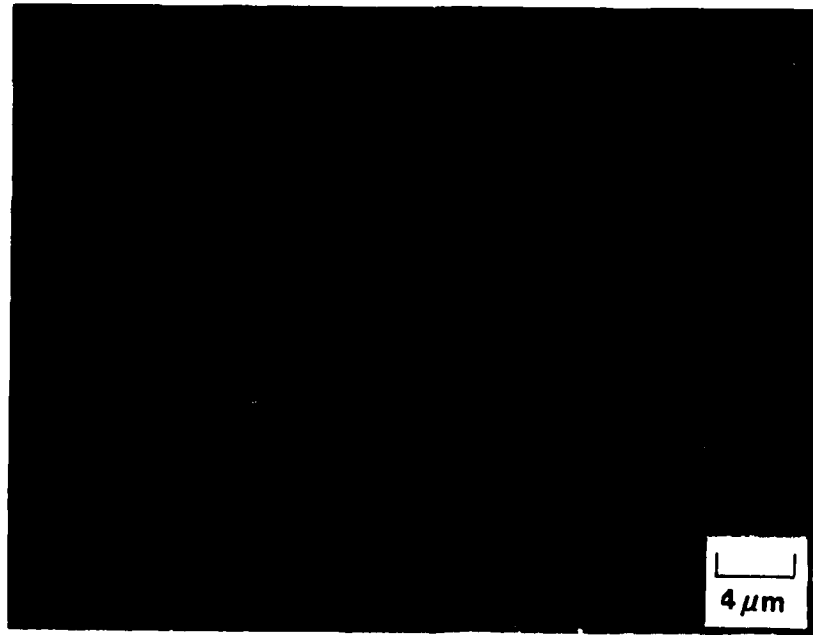


Figure 23. Optical micrographs of shear crack between filaments



H-221



Figure 24. Scanning electron micrographs of shear crack in two-directional carbon-carbon composite



H-223

Figure 25. Micrograph of same shear crack as in Figure 24

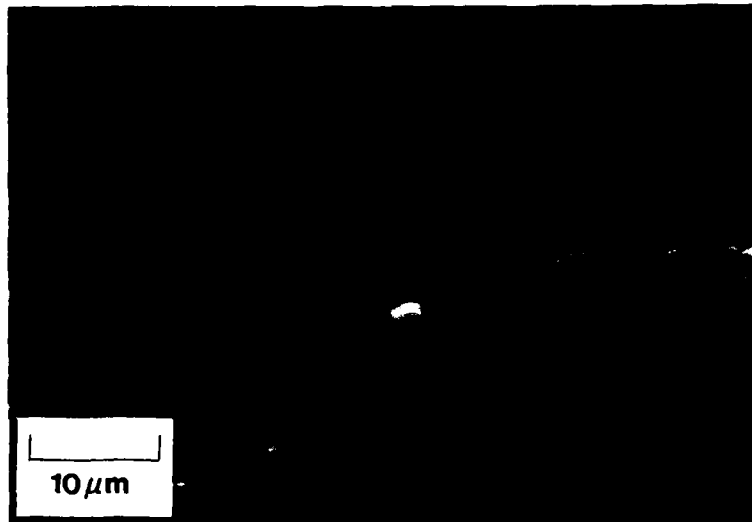
graphite crystallites (original mesophase orientation) is the dominate mode of fracture. Seldom does fracturing occur perpendicular to the crystallites.

In Figure 26, the path of the shear crack was controlled by disclinations of strength $S = -1/2$. These wedge disclinations, shaped like a Y (Figure 2), divert the crack from one branch of the Y to another at an angle near 120° . This angular fracture path occurred at four $S = -1/2$ disclinations in this region. Some exfoliation of the crystallites also occurred. Another segment of a shear crack showing these same features is presented in Figure 27.

A disclination of strength $S = -1$, shaped like an X, is shown in Figure 28. The shear crack followed the outline of this disclination, forcing the crack to change its direction drastically. Within these fiber bundles, only negative wedge disclinations exist¹². The configurations of these disclinations cause crack diverting and crack branching, both mechanisms for energy absorption and increased fracture toughness. The positive wedge disclinations (Figure 2) can cause crack stopping¹².

The angular fracture path produced by cracking through disclinations of strength $S = -1/2$ is shown in Figure 29. Depending on the arrangement of the $S = -1/2$ disclinations, and probably the relative interfacial bond strength at each filament, the fracture path has the tongue-and-groove features (Figure 30) or the angular fracture surface, as in Figure 29.

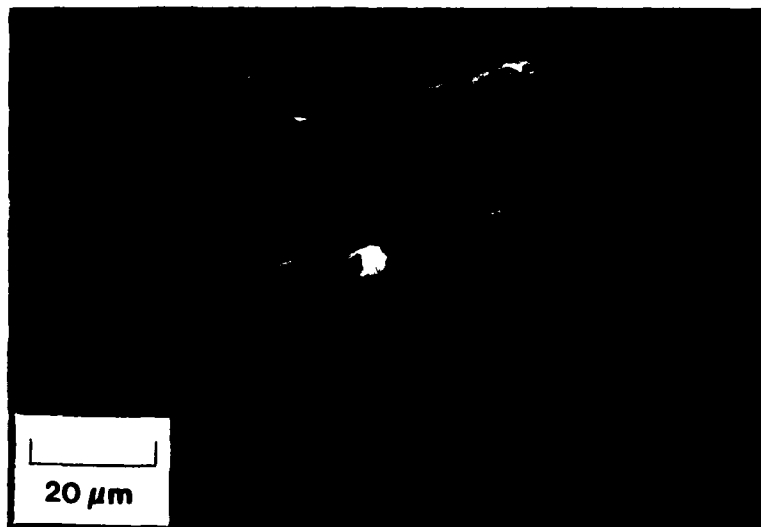
The alignment of the graphitic layers about the filaments is evident in Figure 31. Fracturing at the disclinations and by exfoliation have occurred. The fracturing at the disclinations of strength $S = -1/2$ is illustrated in Figure 32. The remnant matrix on the filaments implies that the strength of the fiber-matrix interface is greater than the cleavage strength of the matrix.



H-226



Figure 26. Micrographs of shear crack among graphite filaments



H-222

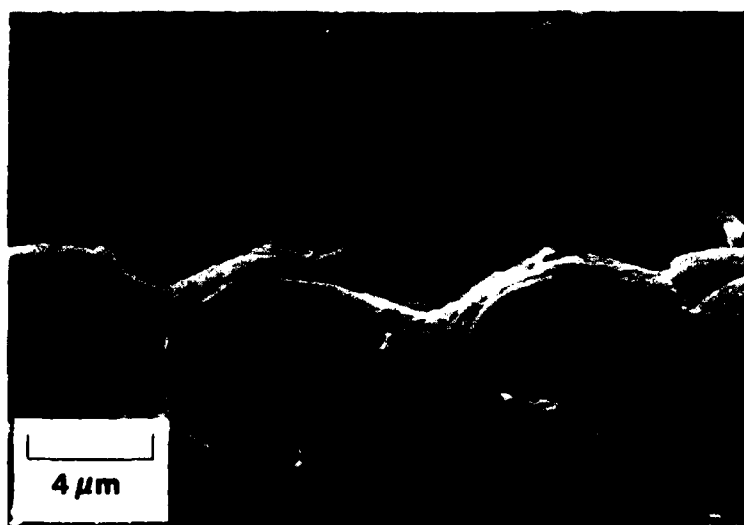


Figure 27. Micrographs of shear crack showing angular fracture surfaces



H-217

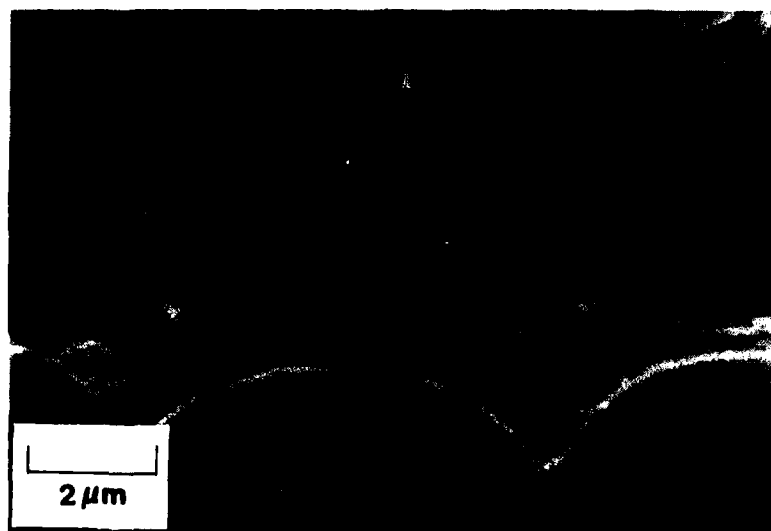
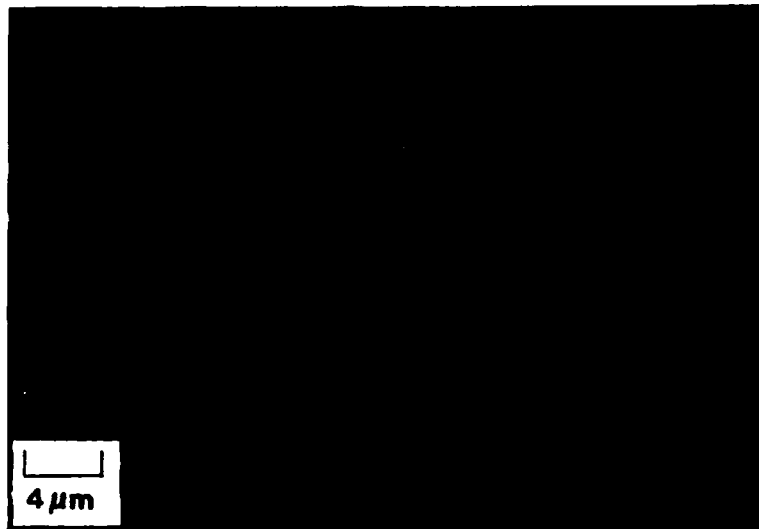


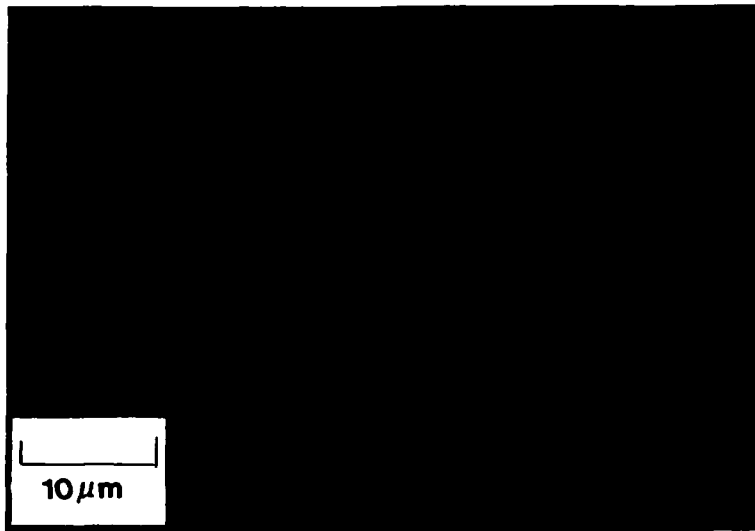
Figure 28. Micrographs of shear crack near disclination of strength $S = -1$



H-218



Figure 29. Micrographs of shear crack showing angular fracture surface at disclinations of strength $S = -1/2$



H-230

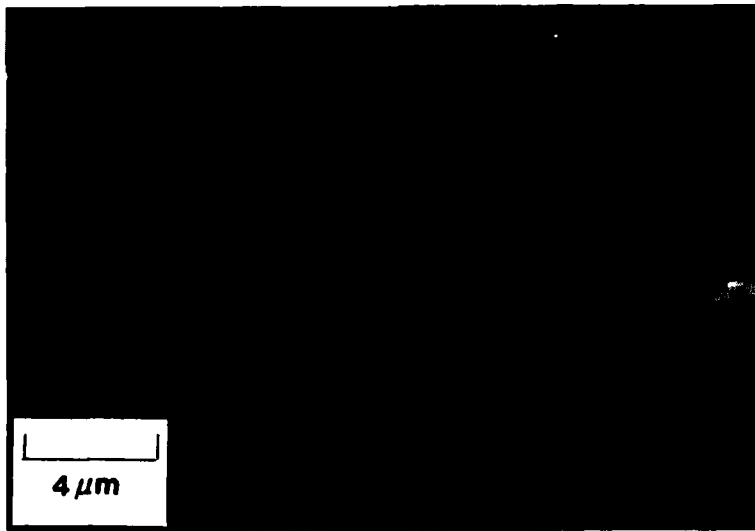


Figure 30. Micrographs of shear crack with tongue-and-groove type of fracturing at the disclinations

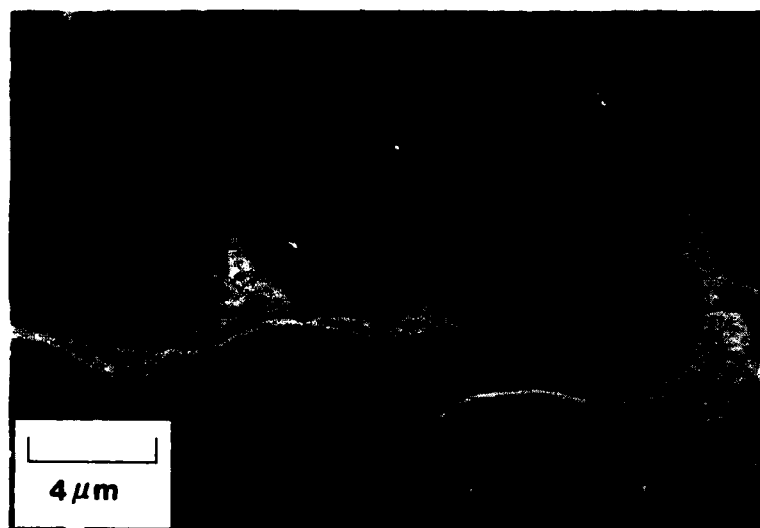
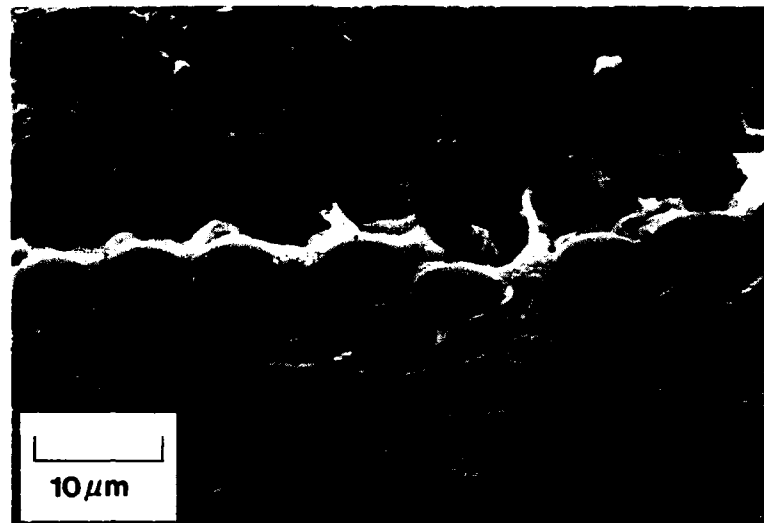


Figure 31. Micrographs of shear crack
at disclinations of strength
 $S = -1/2$



H-231

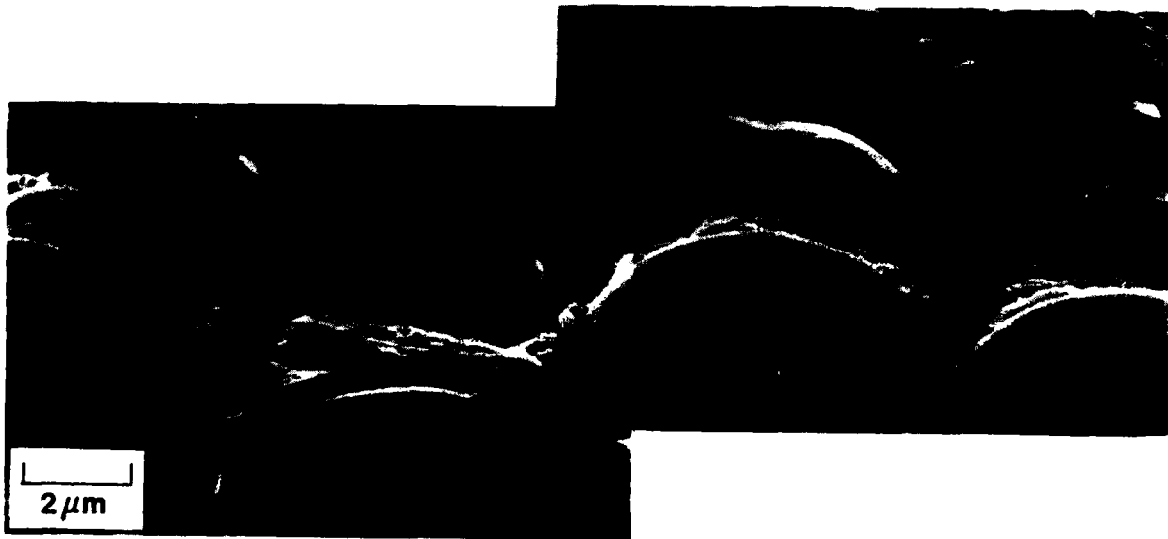


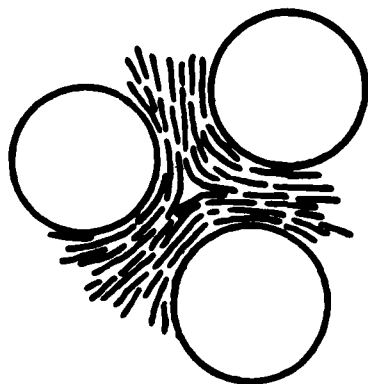
Figure 32. Micrograph of shear crack and $S = -1/2$ disclinations

This optical and scanning electron micrography of shear cracks in a carbon-carbon composite has identified the relation of disclinations to this shear fracturing. The crack path is controlled by the disclinations and is diverted or altered depending on the structure of the disclinations. This type of fracturing, especially the tongue-and-groove type, requires a greater amount of energy than does a simple, straight brittle-type crack. Thus, this tortuous fracturing is a mechanism for increased fracture toughness.

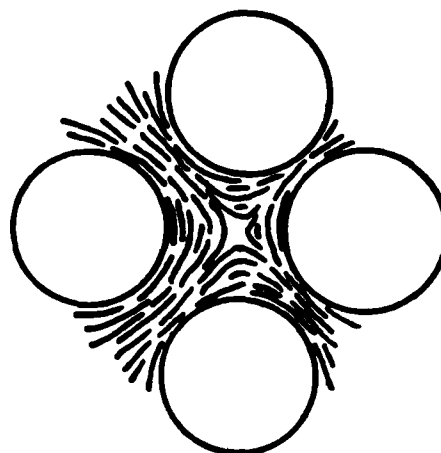
CORE STRUCTURE OF DISCLINATIONS

The types of wedge disclinations which exist among the filaments in a graphite-fiber bundle in a carbon-carbon composite have been identified and characterized in the first annual report¹². The type of disclination is controlled by the arrangement of the filaments, as shown in Figure 33. The alignment of the platelike molecules of the carbonaceous mesophase parallel to the surface of the graphite filaments contributes to this distinct relation between the type of disclination and the type of filament array.

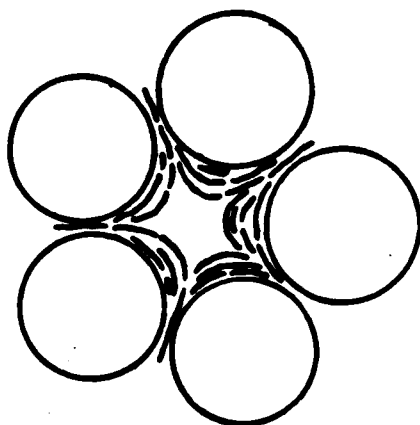
From both theoretical analyses and evidence from optical micrography¹² the core structure of these disclinations were identified as either discontinuous or continuous (Table 1). The core is the small region about the central axis of the wedge disclinations where the stacking of the platelike molecules is forced from the normal, local parallel stacking to a disordered stacking characteristic of each disclination. Topological constraints predict that the cores of the disclinations of strength $S = -1/2$ and $S = -3/2$ are discontinuous. The parallel stacking is retained to the center of the disclination, such that at the molecular level, the central molecules are not stacked parallel. In optical micrography, the discontinuous core of the $S = -1/2$ disclination is characterized by an extinction-contour node which pinches down to a fine point. All the layers about the disclination line remain parallel to the disclination line.



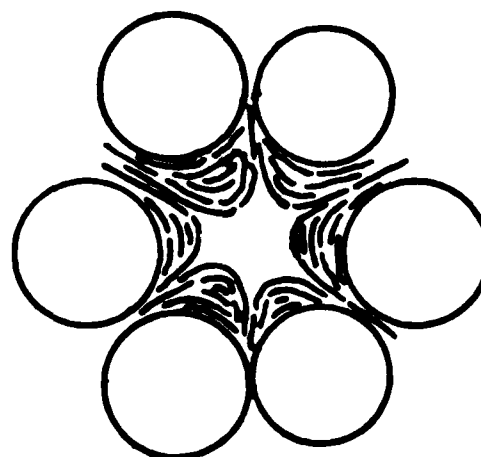
Triangular, $S = -1/2$



Square, $S = -1$



Pentagonal, $S = -3/2$



Hexagonal, $S = -2$

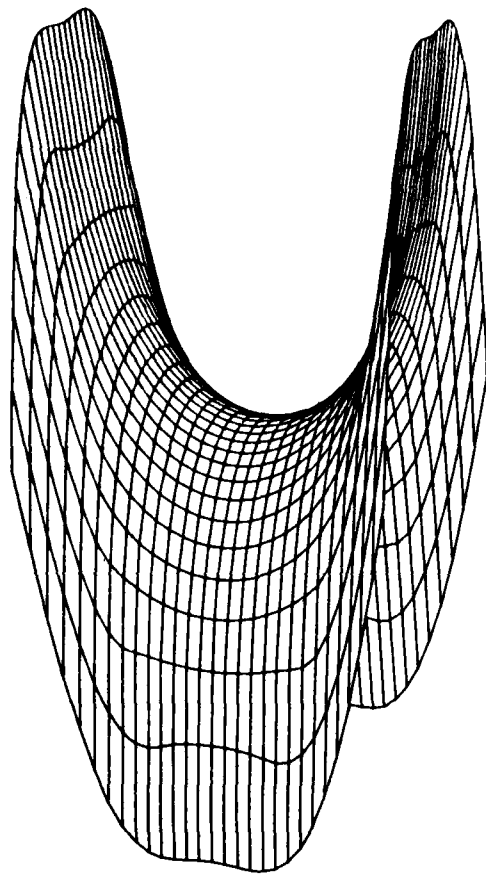
Figure 33. Structure of wedge disclinations in arrays of filaments in a graphite-fiber bundle

Table 1. Disclinations in filament arrays

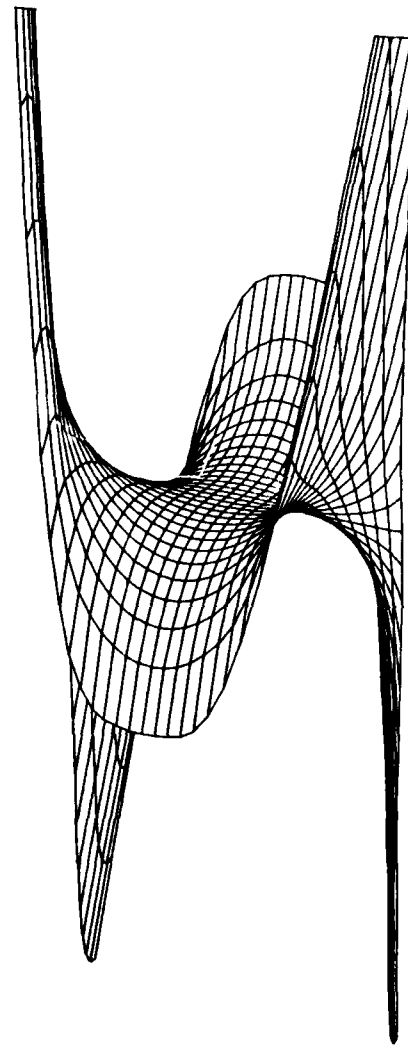
Array	Strength of Disclination	Number of Extinction-Contour Arms	Core Structure	Relative Energy
Triangular	-1/2	2	Discontinuous	1
Square	-1	4	Continuous	4
Pentagonal	-3/2	6	Discontinuous	9
Hexagonal	-2	8	Continuous	16

For the disclinations of strength $S = -1$ and $S = -2$, the core structure is continuous. In these disclinations, the molecular layers in the core change orientation to lie perpendicular to the disclination line. The parallel stacking of the molecules is retained throughout the core. From the theoretical analysis¹² the structure of these cores has been described as shown in Figure 34. Between the four filaments of a square array, the layers map out a saddle-shaped surface. Everywhere the parallel stacking is retained as the adjacent saddle surfaces fit together along the vertical disclination line. For the $S = -2$ disclination, the surface outlined by the molecules in the continuous core is referred to as a monkey saddle. In the optical micrography, these disclinations are characterized by broad, diffuse areas at the intersection of the extinction-contour arms. In bright-field illumination, the brighter response of the core region suggests that the layers are indeed perpendicular to the disclination line, as elsewhere they are parallel to the disclination line.

Although the optical micrography has fully identified the nature of the disclinations in a graphite-fiber bundle, greater resolution of the details of the core structures was needed. Evidence of the distinction between the



Strength $S = -1$,
saddle structure



Strength $S = -2$,
monkey saddle structure

Figure 34. Structure of continuous cores; adjacent surfaces would be stacked vertically along the disclination line

discontinuous and continuous cores would aid in completing the classification and description of these wedge disclinations. Scanning electron micrography was used to identify these core structures. A composite of PAN fibers in A240 petroleum pitch was ion etched with xenon to produce surface relief corresponding to the underlying microstructure of the matrix.

A disclination of strength $S = -1/2$ is shown in Figure 35. All of the graphitic layers are perpendicular to the plane of section and parallel to the disclination line which is nearly normal to the plane of section. The dark lines are graphitization cracks between the graphite crystallites; the light lines are material in ridges on the surface which respond differently in the electron beam. The parallel stacking is retained through the discontinuous core; the actual discontinuity at the center is on a molecular scale beyond the resolution of the scanning electron microscope.

Disclinations in a square array of filaments are shown in Figure 36. Two configurations are possible. There can be either two $S = -1/2$ disclinations present or one $S = -1$ disclination. The total strength of the matrix region among the four filaments of a square array must be -1 . At the core of the $S = -1$ disclinations in Figures 36 and 37, the structure does not appear discontinuous as in the $S = -1/2$ disclination (Figure 35). There is slight evidence of a different orientation of the graphitic layers. A precise outline of the saddle-shaped continuous core is marked by two difficulties. One is the fact that the three-dimensional structure of the saddle structure is not well-defined on a single plane of section. Any evidence of layers parallel to the surface (perpendicular to the line) would help identify the saddle. The other is that the process of graphitization of this composite may have disrupted the continuous layer structure present in the carbonized mesophase. Material may have been removed in polishing or etching. However,

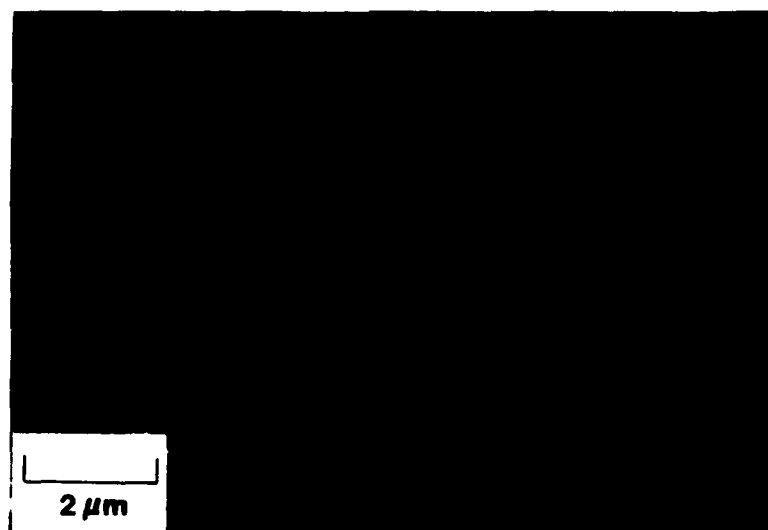
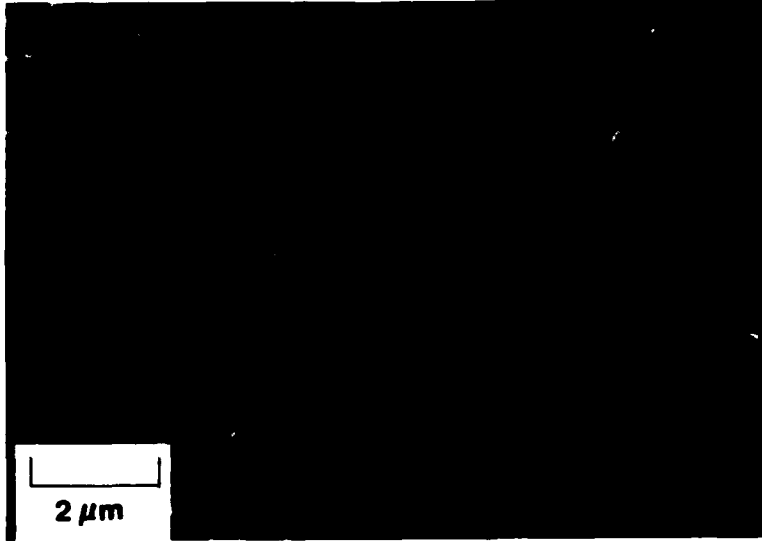
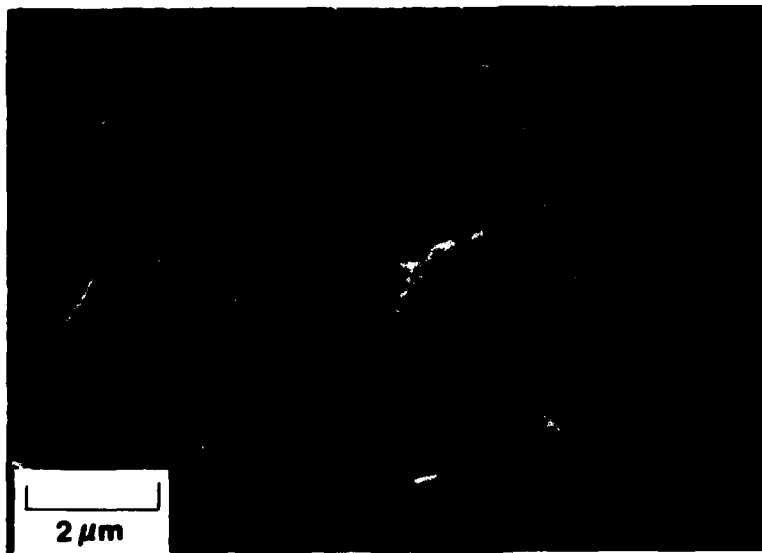


Figure 35. Scanning electron micrograph of disclination of strength $S = -1/2$ with discontinuous core

H-233



2 $S = -1/2$
disclinations



$S = -1$
disclination

Figure 36. Micrographs of disclinations among fibers in square array; (top) two disclinations of strength $S = -1/2$, (bottom) $S = -1$ disclination



H-225

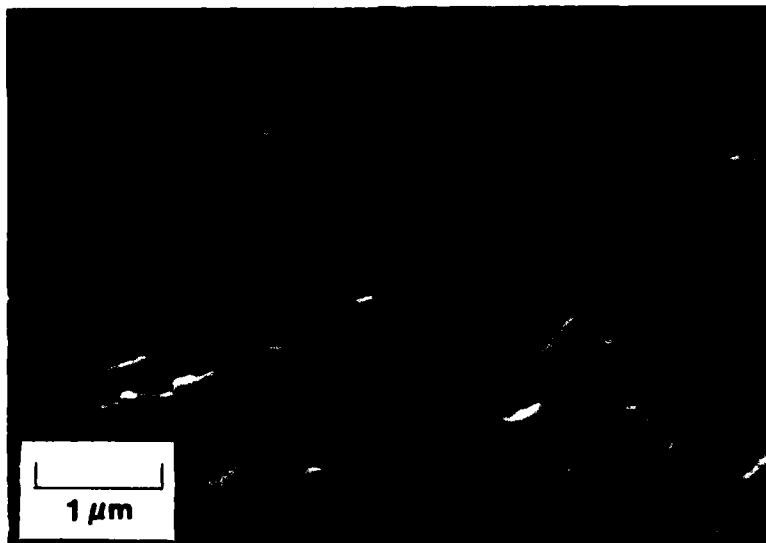


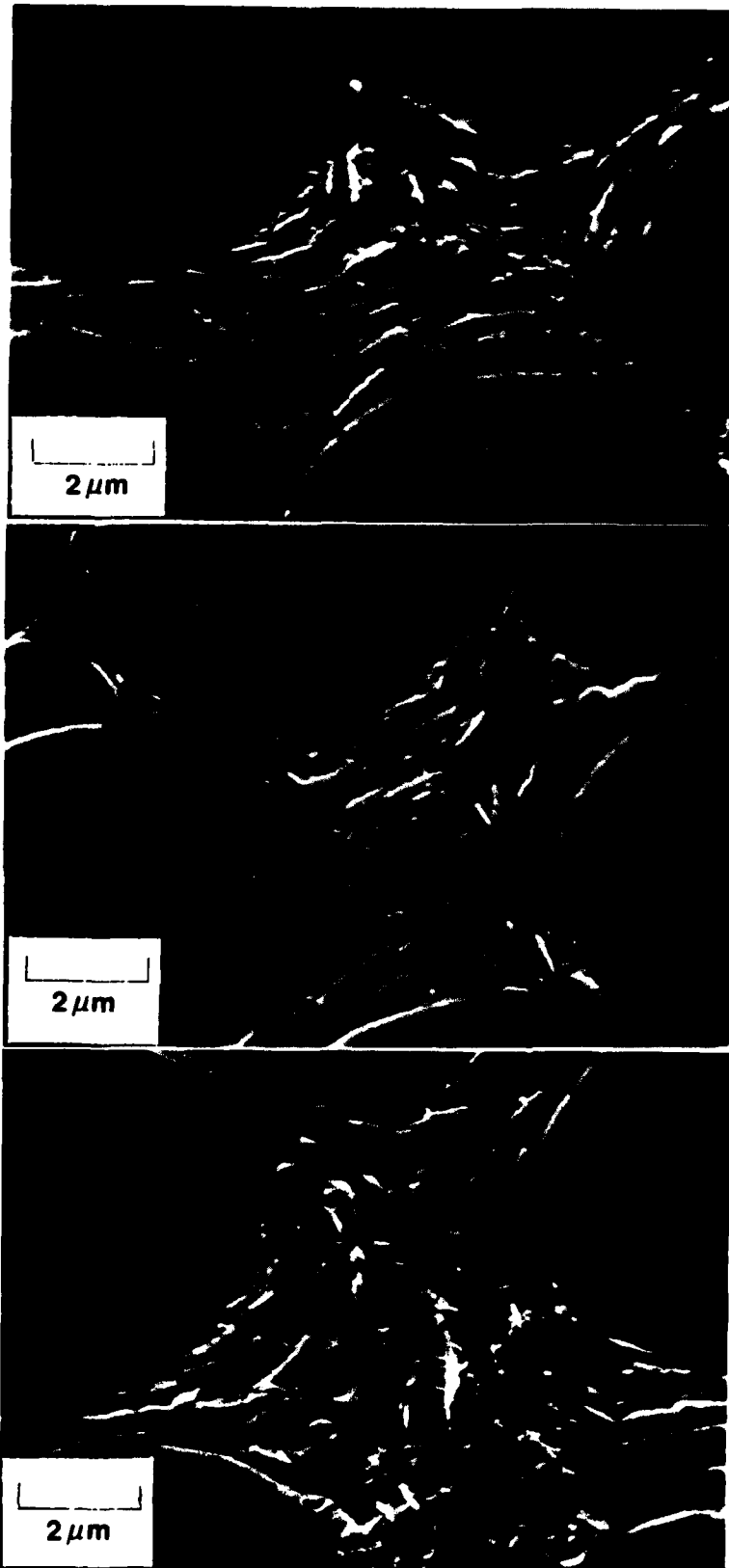
Figure 37. Wedge disclinations of strength $S = -1$ with continuous saddle core

the fact that the core of the $S = -1$ disclination appears more complex than the discontinuous core of the $S = -1/2$ disclination suggests that the core of the $S = -1$ disclination is continuous.

In a pentagonal array of filaments, the total strength for the matrix is $-3/2$. The matrix can contain a single disclination of strength $S = -3/2$ or several disclinations of lower strength which total $-3/2$. Since the energy of a disclination is proportional to the square of its strength (Table 1), several disclinations of lower strength is energetically favorable over one $S = -3/2$ disclination. Examples of several disclinations in the matrix in a pentagonal array are shown in Figure 38. The occurrence of the $S = -3/2$ disclination is not frequent. One such disclination is shown in Figure 39. This is identified as an $S = -3/2$ disclination as no $S = -1/2$ or $S = -1$ disclinations are present. The $S = -3/2$ disclination should have a discontinuous core. This particular core is not well defined; there appears to be a triangular shaped ridge of material at the core. The search for a clearer example of the $S = -3/2$ disclination will continue.

Several disclination arrays which are present in the matrix in a hexagonal array of filaments are shown in Figure 40. These occur more frequently than a single disclination of strength $S = -2$. A disclination of strength $S = -2$ is shown in Figure 41. The core of this disclination should be like the monkey saddle. There appears to be such a core in this disclination. It is Y-shaped and each segment of the Y appears to be a trough with layers parallel to the surface at the bottom of the trough and curving upward along the sides of the trough. In between the Y segments, the layers should be curving downward to complete the continuous monkey-saddle core. The curvature in this core occurs over a distance of about $0.5 \mu\text{m}$; finer

H-235



$S = -1/2, S = -1$
disclinations

$3 S = -1/2$
disclinations

$3 S = -1/2$
disclinations

Figure 38. Disclinations among fibers in pentagonal array of equivalent strength $S = -3/2$

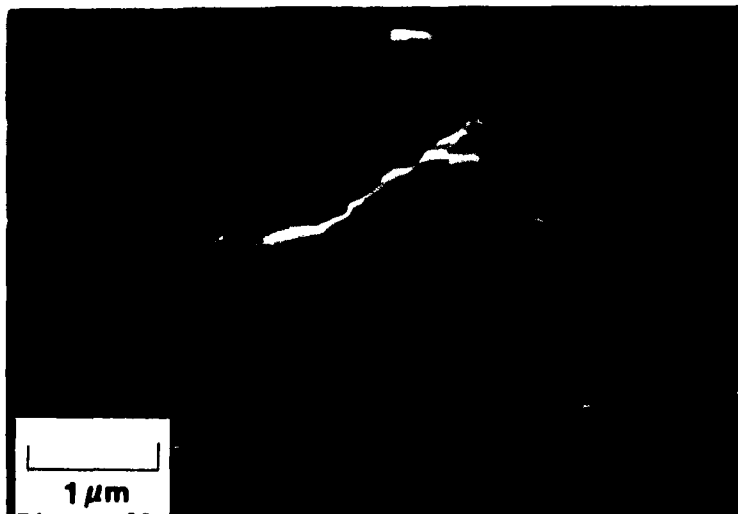
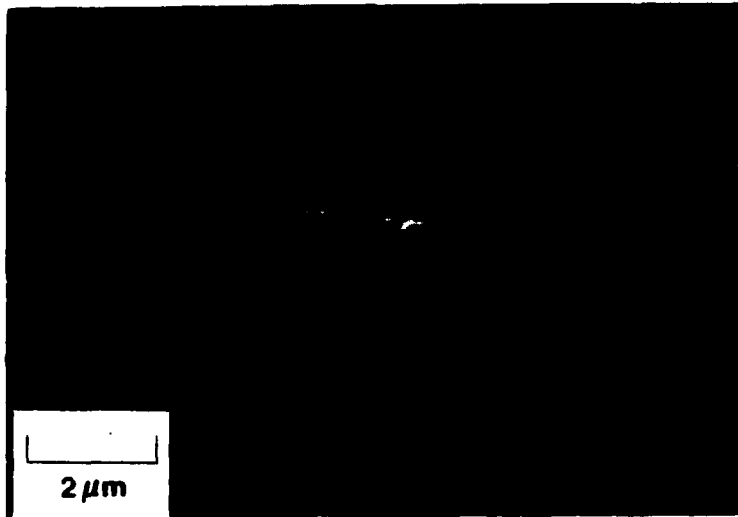
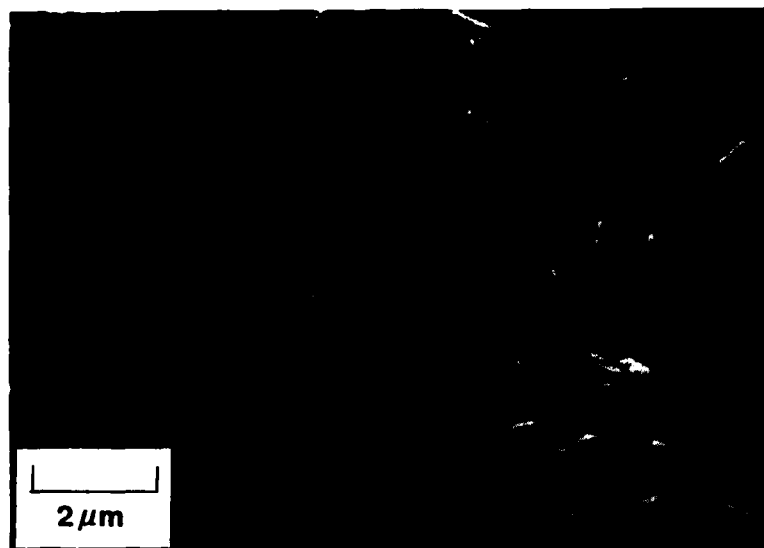
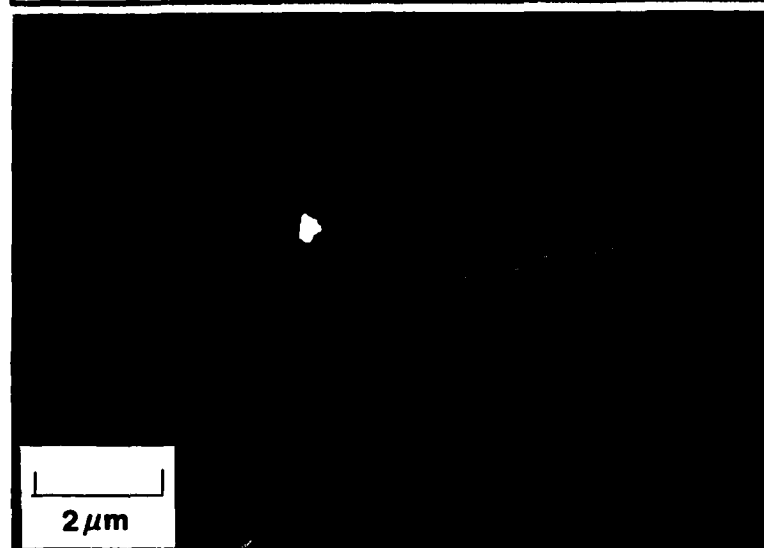


Figure 39. Discrimination of strength $3 \pm 1/2$ in pentagonal array; specimen was rotated about normal to surface in top two micrographs

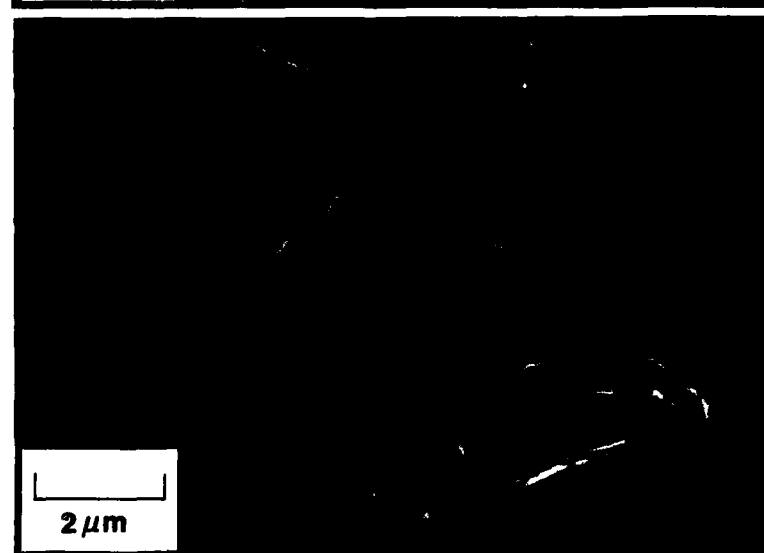


H-224

4 $S = -1/2$
disclinations



2 $S = -1/2$,
 $S = -1$
disclinations



4 $S = -1/2$
disclinations

Figure 40. Disclinations among fibers in hexagonal array of equivalent strength $S = -2$



H-256

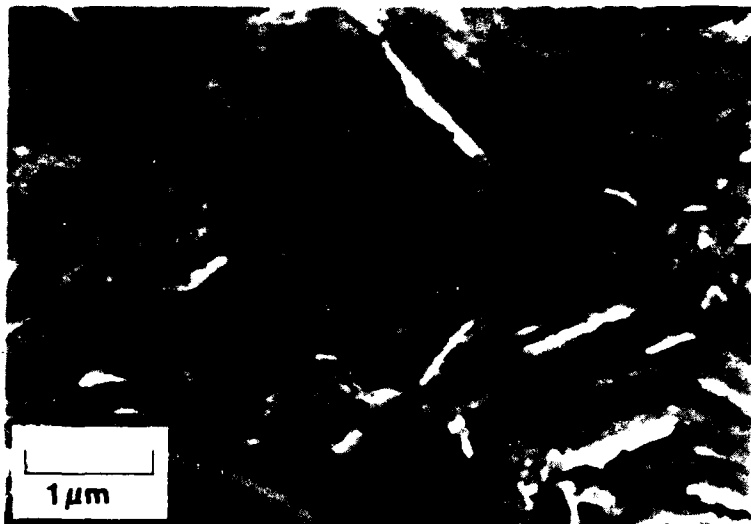


Figure 41. Disclination of strength $S = -2$ in hexagonal array; disclination has continuous core shaped like monkey saddle

resolution of this core is beyond the capability of this scanning electron microscope.

This identification of the types of disclinations and their core structures in a graphite-fiber bundle is a necessary first step to understanding the complex fracture behavior of carbon-carbon composites. Fracturing in a fiber bundle was shown in this report to be controlled by the disclinations. The core structure of the disclinations may contribute to this fracturing as sketched in Figure 42. The crack path through a disclination with a discontinuous core will be diverted along a path with a single plane of curvature. But a crack through a disclination with a continuous core must follow a more tortuous path with double curvature.

Controlling the matrix microstructure of a carbon-carbon composite during its formation via the carbonaceous mesophase may result in improved fracture toughness. Other physical properties such as thermal expansion and elastic modulus may reflect changes in the matrix microstructure. Research during the next year will be aimed at studying the effects of a magnetic field on mesophase alignment and disclination structures. The carbonaceous mesophase can be aligned by a magnetic field⁵. The normals to the platelike molecules orient perpendicular to the direction of the magnetic field. The effect of the magnetic field on the mesophase transformation will first be investigated. The influence on mesophase nucleation and spherule formation and coalescence will be studied. Second, the influence of the magnetic field on the disclination structures in a fiber bundle will be studied for different angles between the direction of the magnetic field and the axis of the fiber bundle. The changes in the disclination arrays will be observed with optical and scanning electron microscopy.

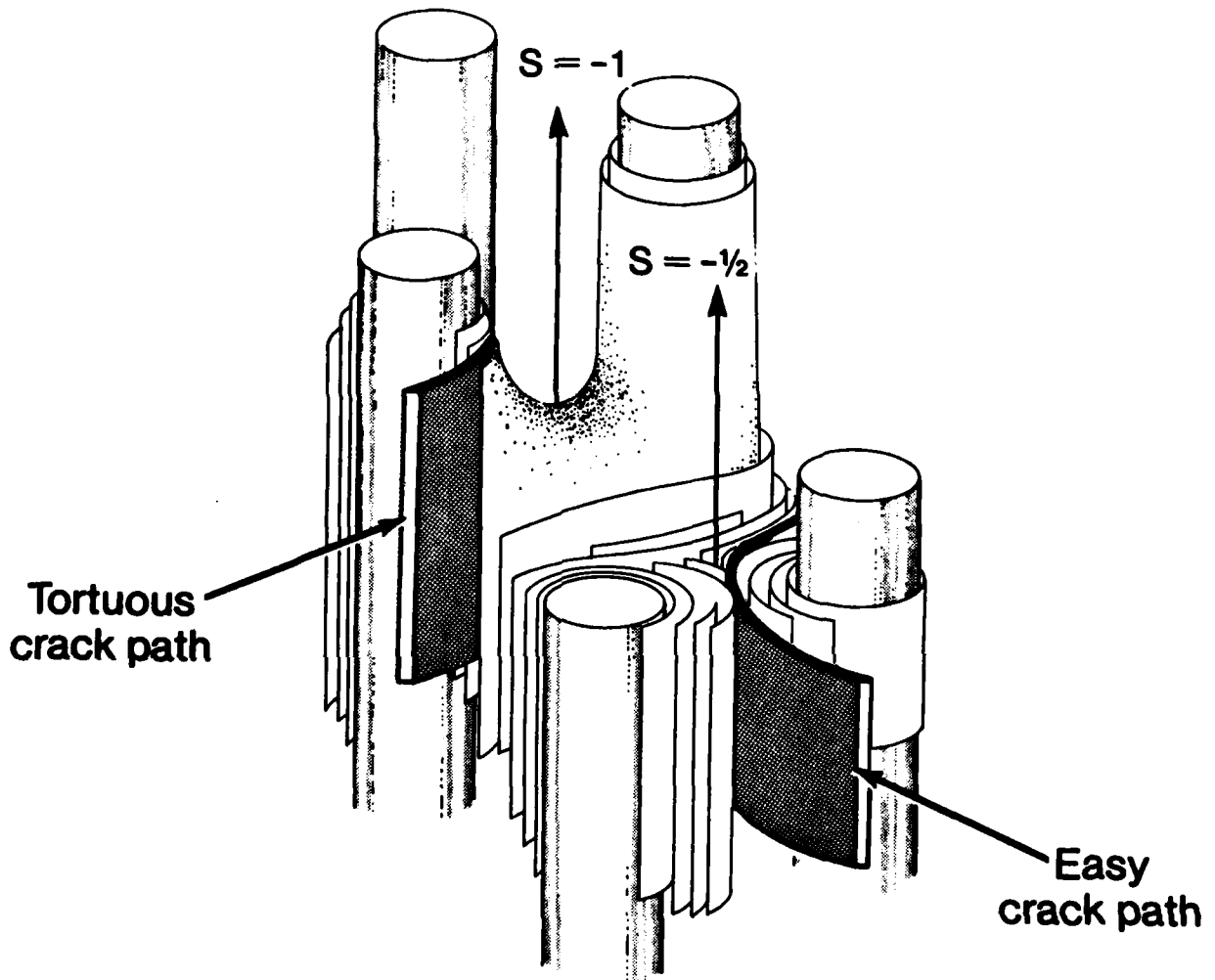


Figure 42. Schematic diagram of fracturing in a graphite-fiber bundle

PUBLICATIONS

The following technical publications have been prepared with support in part by this research program:

1. J. E. Zimmer and J. L. White, Carbon 21, 323 (1983): a letter to the editor entitled "Mesophase Alignment Within Carbon-Fiber Bundles."
2. J. E. Zimmer, "Disclinations and Fracture," presentation at International Symposium on Carbon, 1-4 November 1982, Toyohashi, Japan.
3. J. E. Zimmer and R. L. Weitz, Extended Abstracts, 16th Conference on Carbon, p. 92 (1983): a paper entitled "Disclinations in a Graphite-Fiber Bundle."

complex permittivity resolution of the measurement system is directly proportional to the specimen capacitance. We have repeated the experiment five times and the mean value has been used to plot the experimental results.

The experimental results for ϵ' and ϵ'' vs log frequency are shown in Figs 1 and 2. The imaginary part (ϵ'') of the complex permittivity increases rapidly with increasing carbon concentration in rubber. The real part (ϵ') of the complex permittivity shows anomalous dispersion with frequency and its value increases with the increase in carbon concentration specially in the low frequency region. ϵ'' increases over a frequency range 10^1 to 5×10^4 Hz and decreases afterwards. ϵ' decreases with frequency very rapidly in a frequency range 10^1 - 10^3 Hz. Figure 2 shows that an absorption is maximum at 5×10^4 Hz. ϵ'' of the complex permittivity of the mixture is of great importance at low frequency where absorption is maximum.

This type of material is very useful for low frequency

absorption. The absorption capability of the material increases with carbon concentration. This material may be used to construct special types of chamber to absorb radiated power above the communication frequency band for specialised applications.

Antenna Engineering
Spar Aerospace Ltd.
21025 Trans Canada Highway
Ste-Anne-de-Bellevue
Quebec
Canada H9X 3R2

A. KUMAR

References

1. A. Kumar, *Carbon* 18, 231 (1980).
2. Imperial Chemical Industries Ltd., British Patent Applications 1316169 and 25945 (1970).
3. A. Kumar, Unpublished work.

Carbon Vol. 21, No. 3, pp. 323-324, 1983
Printed in Great Britain

0008-6223/83 \$3.00 + .00
Pergamon Press Ltd.

Mesophase alignment within carbon-fiber bundles

(Received 12 November 1982)

The tendency for layers of carbonaceous mesophase to align parallel to the surface of substrates, such as graphite flakes, coke particles and ceramic materials, was recognized early [1, 2]. This alignment is inherent in the fiber bundles of carbon-carbon composites, which consist of graphitic matrices formed via the mesophase and reinforced by high-modulus carbon filaments. Circular mesophase sheaths, at least several microns in thickness and extending the length of each filament, are normally found on carbon filaments made from rayon, polyacrylonitrile, or mesophase pitch. The latter case is of special interest because some mesophase pitch filaments have the radial open-wedge structure that appears in Fig. 1: graphitic layer faces are exposed in the open wedge while the periphery of the filament is composed of layer edges [3]. Cranmer *et al.* [4] found that, when a petroleum or coal-tar pitch is pyrolyzed within such a fiber bundle, the mesophase formed in the early stages of transformation preferentially wets the graphitic layers of the open wedge. We have observed that when full transformation is achieved by further pyrolysis, as is the case for Fig. 1, the mesophase layers are aligned parallel to both open-wedge and

peripheral surfaces, independent of the orientation of the graphitic layers of the substrate.

Within a bundle of carbon filaments, the alignment of the mesophase as a circular sheath about the filaments prescribes, to a large extent, the mesophase morphology throughout the remaining volume of the filament array. Each sheath effectively constitutes a positive wedge disclination of strength $S = +1$, where $2\pi S$ is a measure of the rotational distortion of the disclination [5]. To

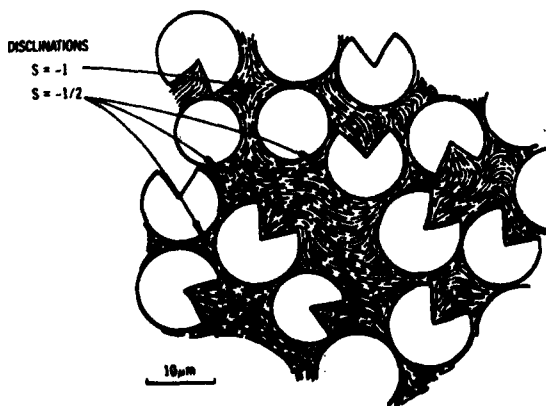


Fig. 1. Alignment of carbonaceous mesophase within a bundle of carbon filaments. The radial open-wedge filaments were spun from mesophase pitch. Section transverse to axis of filament bundle; sketch is mapped by polarized-light micrography with immersion oil.

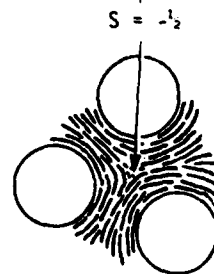
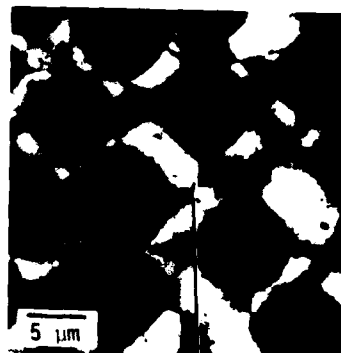


Fig. 2. Wedge disclination of strength $S = -\frac{1}{2}$ in triangular array of carbon filaments. Section normal to polyacrylonitrile-carbon filaments in mesophase from A240 petroleum pitch heated at 400°C for 24 hr; polarized-light micrography with immersion oil.

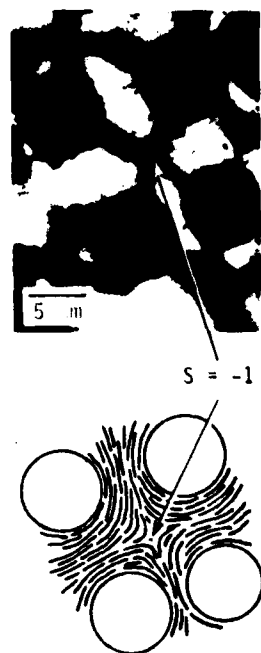


Fig. 3. Wedge disclination of strength $S = -1$ in square array of carbon filaments. Same conditions as Fig. 2.

maintain the balance of disclination strengths required of a liquid crystalline body[6], the matrix among the filaments must contain predominantly negative wedge disclinations, as is seen to be the case for Fig. 1. For an array of parallel filaments, the sum of the strengths of the sheaths ($S = +1$) and the wedge disclinations ($S = -\frac{1}{2}, -1$) tends to zero.

We have also found that the type of negative wedge disclination is determined by the local packing of filaments. This is best shown for the round filaments (polyacrylonitrile-based) of Figs. 2 and 3. When the filaments are quite closely packed to form a triangular array, the intervening matrix contains a wedge disclination of strength $S = -\frac{1}{2}$. When the filaments comprise a square array, the matrix contains a wedge disclination of strength $S = -1$. The $S = -1$ disclinations at equilibrium have saddle-shaped continuous cores (Fig. 4) in which the parallel stacking of the mesophase layers is retained throughout the disclination core[7]. This continuous core reduces the energy of the disclination line[8]. Due to their geometry, the $S = -\frac{1}{2}$ disclinations must have discontinuous cores. Thus, the effect of the coincidence of the strong mesophase alignment on filaments in a square array and this saddle-shaped core structure is that the mesophase layers in a small region near the center of the array are aligned perpendicular to the filaments.

Acknowledgement—The authors thank the Office of Naval Research for support of this work.

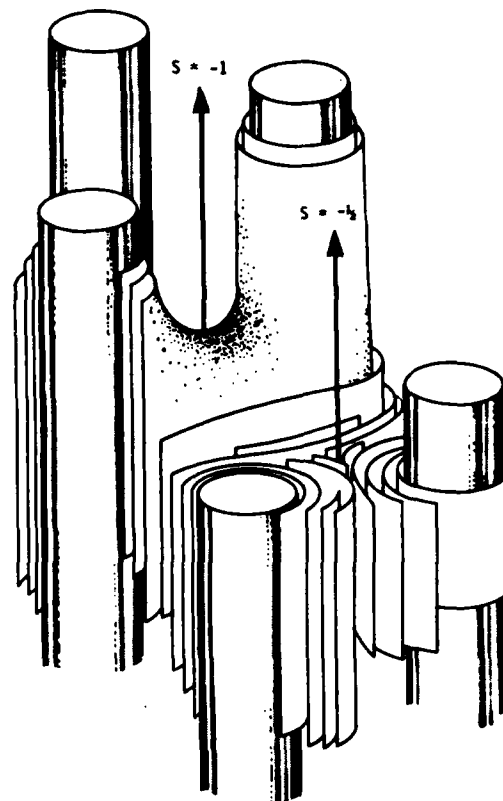


Fig. 4. Disclinations of strength $S = -\frac{1}{2}$ and $S = -1$ in proximity in a fiber bundle. The mesophase layers align parallel to the carbon filaments, but lie perpendicular to the filaments in the continuous core of the $S = -1$ disclination.

Acurex Corporation
Mountain View
CA 94042
U.S.A.

J. E. ZIMMER

The Aerospace Corporation
El Segundo
CA 90245
U.S.A.

J. L. WHITE

REFERENCES

1. J. D. Brooks and G. H. Taylor, *Carbon* 3, 186 (1965).
2. J. Dubois, C. Agace and J. L. White, *Metallography* 3, 337 (1970).
3. L. S. Singer, *Carbon* 16, 408 (1978).
4. J. H. Cranmer, I. G. Plotzker, L. H. Peebles, Jr. and D. R. Uhlmann, *Carbon* in press.
5. J. L. White and J. E. Zimmer, *Surface and Defect Properties of Solids* 5, 16 (1976).
6. J. Nehring and A. Saupe, *J. Chem. Soc., Faraday Trans.* 68, 1 (1972).
7. J. E. Zimmer and J. L. White, *Extended Abstracts, 14th Conf. on Carbon*, p. 429 (1979).
8. R. B. Meyer, *Phil. Mag.* 27, 405 (1973).

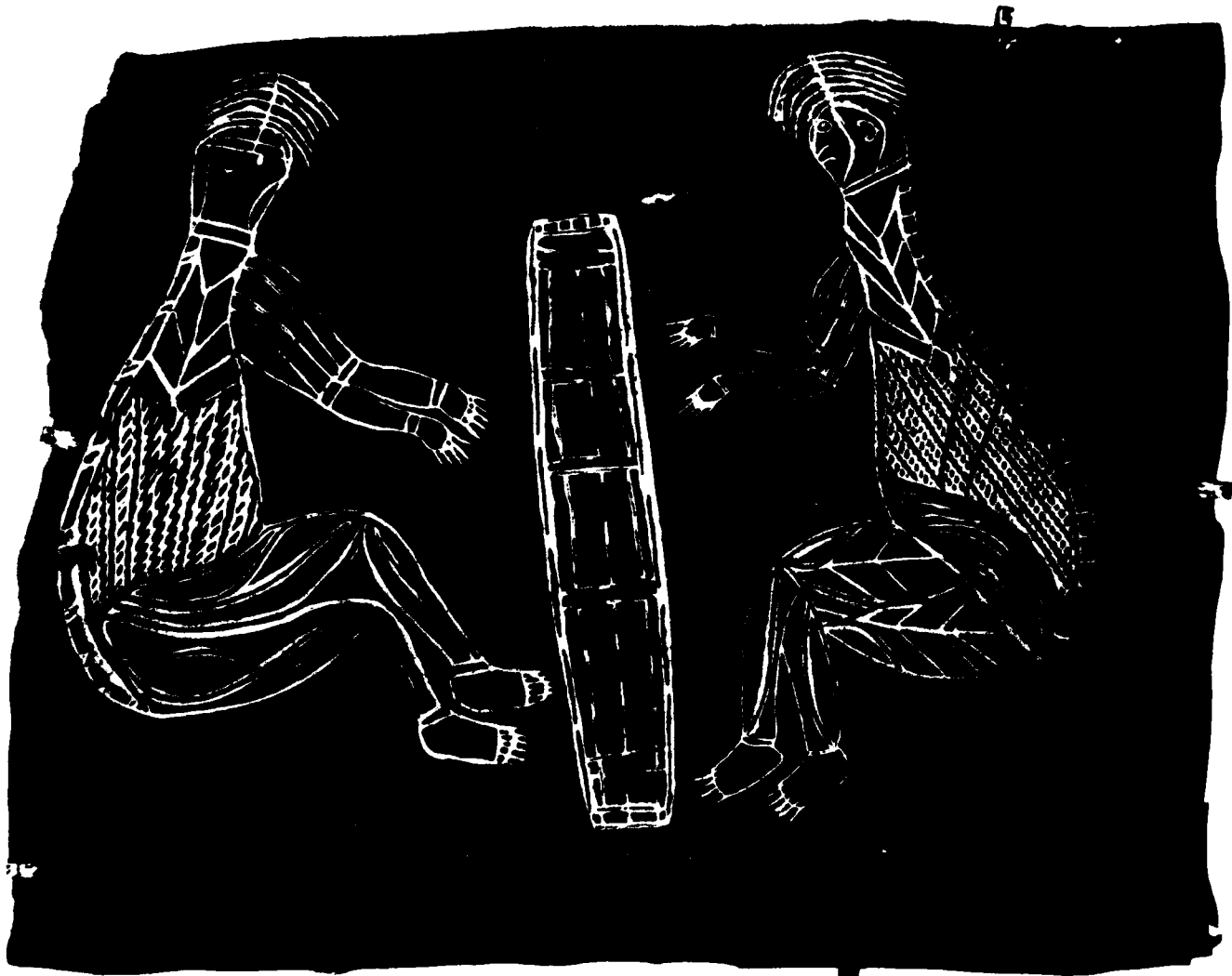
REPRINTED FROM
JANUARY TO MARCH 1983

VOL. 8, NO. 1

SCIENTIFIC BULLETIN



DEPARTMENT OF THE NAVY OFFICE OF NAVAL RESEARCH FAR EAST



NAVSO P-3580

INTERNATIONAL SYMPOSIUM ON CARBON

Jim Zimmer

INTRODUCTION

The International Symposium on Carbon: New Processing and New Applications was held in Toyohashi, Japan on 1-4 November 1982. This was the second international carbon conference sponsored by the Carbon Society of Japan, the first being held in 1964. The number of attendees was 353 with 51 from overseas. A total of 148 technical papers were presented in both oral and poster sessions. The organizing committee included:

- Professor H. Honda, Science University of Tokyo. Chairman,
- Professor T. Tsuzuku, Nihon University, Vice-Chairman,
- Professor S. Otani, Gunma University. Secretary-General,
- Professor H. Suzuki, Tokyo Institute of Technology, Treasurer
- Professor Y. Sanada, Hokkaido University, Technical Program Leader, and
- Professor M. Inagaki, Toyohashi University of Technology, Local Arrangements Leader.

This committee deserves commendation for the well-run and technically informative symposium.

Carbon is a unique and important material. Its many uses include polycrystalline graphite for electrodes in steel and aluminum making and for the moderator in gas-cooled nuclear reactors, carbon fibers for the reinforcement and strengthening of polymers for such applications as sporting goods and airplane components, and carbon materials for endoprosthetic joints and dental implants. The topic areas of this symposium were as follows:

- New Processing
 - raw materials preparation
 - mesophase control
 - manufacturing methods
 - characterization and design
- New Applications
 - nuclear carbon
 - carbon fiber
 - intercalation compounds
 - biocarbons and potential uses
- Fundamentals
 - physics
 - chemistry
 - technology

The technical presentations covered all aspects of carbon technology from basic research to industrial applications, as exemplified in the plenary lectures presented:

S. Ootani Gunma University Japan	Development of carbon technology in Japan
K. J. Huttinger University of Karlsruhe West Germany	Carbon materials for endoprosthetic joints
H. Juntgen Bergbau-forschung GmbH West Germany	Basic reactions and technical performance of coal gasification and liquefaction
B. T. Kelly United Kingdom, Atomic Energy Authority England	The control of irradiation damage in graphite
T. Tsuzuku Nihon University Japan	Studies on electric processes in graphite during the last decade in Japan
H. P. Boehm University of Munich West Germany	Graphite intercalation compounds: old and new problems in the chemist's view
L. S. Singer Union Carbide Corporation U.S.A.	Carbon fibers from mesophase pitch: past, present, and future
R. Setton Centre de Recherches sur les Solides à Organisation Cristalline Imperfaite France	The organic chemistry of some intercalation compounds of graphite

This report will center on the advances in carbon fibers, specifically mesophase-pitch fibers, the carbonaceous mesophase and its role in carbon materials, and the use of carbon materials for dental implants and prosthetic joints.

CARBON FIBERS

Most carbon fibers are made from the polymer precursors, rayon and polyacrylonitrile (PAN). The amount of carbon fiber from PAN produced in Japan is about 500 tons a year. These fibers offer either high strength or high modulus, depending on the level of heat treatment. The invention and production by L. S. Singer and his coworkers at the Union Carbide Corporation, U.S.A., of carbon fibers from pitch have demonstrated that carbon fibers can offer both high modulus and strength. The precursor for these pitch fibers is either petroleum pitch or coal tar pitch which is heated to between 400° and 500°C to form the carbonaceous mesophase, a discotic nematic liquid crystal. The spinning of this orientable liquid crystal provides the high degree of alignment of the graphitic structure in the resulting carbon fiber and thus its high modulus. Essential factors for successful production of these mesophase-pitch carbon fibers are low viscosity at low melt-spinning temperatures, agitation and gas sparging of the mesophase before spinning, and removal of

ash or infusible carbonaceous solids. Processing includes spinning, infusibilizing, carbonizing, and graphitizing. Elastic moduli range from 25×10^6 to 100×10^6 psi. Union Carbide now produces 250 tons a year. New applications of this low-cost carbon fiber include structures in outer space which require high stiffness and strength, and low thermal expansion.

A mesophase-pitch carbon fiber is not yet on the market in Japan. But there is much interest on the part of many researchers in Japan in understanding the spinning and production of these mesophase-pitch fibers. The precursors for these fibers are quite abundant in Japan: petroleum pitch from oil refining and coal tar pitch from coking coals used in blast furnaces for steel making. Several companies in Japan that are undertaking research on mesophase-pitch fibers are the Nippon Steel Corporation, the Kawasaki Steel Company, Tonen Oil Company, Mitsubishi Chemical Industries, Ltd., the Kureha Chemical Company, and Mitsui Coke Company.

Intercalation compounds of graphite crystals with a high degree of crystal perfection show metallic electrical conduction comparable to that of the metal, copper. The intercalation compounds formed by using graphite fibers could afford high potential for application as an electroconductive wire for high-power transmission lines or aircraft where light weight is needed. M. Endo, Shinshu University and T. Koyama and M. Inagaki, Toyohashi University of Technology, have shown that by intercalation with HNO_3 , K and AsF_5 , the resistivity of a graphite fiber was reduced from 80 to less than $2 \mu\Omega$ -cm.

Another exciting area of research in carbon fibers is the fabrication of vapor-grown carbon fibers. Professor M. Endo, Shinshu University, in conjunction with Showa Denko Company, Ohmachi, has developed vapor-grown carbon fibers by means of thermal decomposition of hydrocarbons with seeding by catalytic ultrafine particles of metals. Cylindrical substrates, seeded with iron or iron-nickel particles about 10 to 50 nm in diameter, were heated at temperatures about 1000° to 1250°C in a mixture of vaporized benzene and hydrogen gas. The resulting fibers consist of concentric stacked layers of carbon planes with a hexagonal network about the fiber axis. There is a small hollow core. This seeding method is effective in producing a large quantity of vapor-grown carbon fibers with high reproducibility and controlled dimensions. The method is applicable to an automatic production system, which could afford one of the simplest production methods for carbon fibers.

Professor M. Egashira and his co-workers at Nagasaki University have prepared vapor-grown fibers from the thermal decomposition of benzothiophene and Z-thionaphthol at 1100° to 1300°C . The sulfur in these organic molecules promotes the growth of the fibers. The particle which nucleated the growth was SiC; the Si was present in the mullite substrate. Small particles and temperatures near 1100°C produced long, thick carbon fibers with a yield of five percent.

CARBONACEOUS MESOPHASE

The carbonaceous mesophase is a liquid crystal formed during the pyrolysis of polynuclear aromatic hydrocarbons such as petroleum pitch, coal tar pitch and naphtha-cracked tar. In the temperature range of 400° to 500°C , microstructures introduced in the carbonaceous mesophase are retained in the graphitic materials formed from this liquid crystal. Thus, much research is being conducted in Japan, as well as in the United States, England, Germany, and France, on the chemistry and physics of the carbonaceous mesophase, the precursor to polycrystalline graphite and the mesophase-pitch fibers.

T. Miyazaki, Mitsubishi Chemical Industries, Ltd., discussed the development of needle coke from coal tar pitch. Needle coke, which consists of well-developed, needle-shaped crystals of carbon, is the starting material for ultra high-power graphite electrodes. As the demand for such sophisticated electrodes increases, the critical problems of expanding the volume of production and upgrading the quality of needle coke to meet technical needs have to be solved. However, only selected heavy petroleum oil with low sulfur, low ash, and low asphaltene contents has been believed to be suitable for manufacturing needle coke. If this is to continue in the future, there will be danger in a shortage of the raw material supply to meet the sharply growing demand. In addition, the threat posed by the prevailing instability in the world oil situation urgently requires that new sources of feed stock be examined in order to ensure an abundant and stable availability of raw material. Under such circumstances, Mitsubishi Chemical Industries and the Nittetsu Chemical Industrial Company have been developing methods of manufacturing needle coke from coal tar pitch. For coal tar pitch containing a high concentration of fine, inert particles, mesophase formation and deformation to produce the required needle coke is impeded. Removal of the fine particles has been accomplished by the use of solvents to coagulate the particles to cause precipitation and separation. The graphite electrodes produced from the needle coke from coal tar pitch were of good quality and were characterized by low spalling and low graphite consumption. Such a coal tar pitch could also be used for mesophase-pitch fibers.

Related research is being done by Professor I. Mochida, Kyushu University. To utilize the precious petroleum completely, the bottoms of the barrel are expected to be converted to carbon materials such as needle coke or carbon fiber. Among various residues, the tar produced in the naphtha cracking for ethylene production consists of principally aromatic hydrocarbon, so that it is a prominent resource of carbon precursors, although it requires considerable modification because of low coking value. Acidic modification using the least amount of aluminum chloride has been accomplished for the conversion of these tars to sources for needle coke and carbon fiber precursors.

In the production of coke for steel blast furnaces, high-rank, nonfusible coals can be used as coke only if their fusibility and strength are improved. The improvement of the fusibility of such coals by adding coal tar pitch, petroleum pitch, or solvent-refined coal has been accomplished by T. Abe and his coworkers at the Kansai Coke and Chemicals Company. Important in this blending of pitch and coal is the role of transferable hydrogen. T. Obara, Hokkaido University, has shown the transferable hydrogen is influenced by Lewis acids and atmospheric oxidation and is one of the keys to controlling the carbonization reactions of coals and pitches.

BIOCARBONS

Carbon has excellent biocompatibility with the human body and thus has found application as dental implants, heart valves, and bone prostheses. Dental implants with a fine Rahmen surface are prepared by low temperature pyrolytic carbon deposition on carbon substrates. This process was developed by A. Kojima, Gunma Technical College; S. Ohtani, Gunma University; and S. Yanagisawa, the School of Dentistry, Nihon University. Preclinical tests have shown that implants in primate jaws under loading for two years performed excellently. In the surface structure of the implant, collagen fiber bundles were interwoven with the carbon implant and deeply ingrown tissue was ossified and filled all spaces of the surface structure. The implant brought about a hybrid load-transmitting system of carbon and bone. Thus, the implant can be used as an artificial replacement of the skeletal defect or loss of dentition that needs strong attachment to living tissue. The use of carbon materials for endoprosthetic joints was presented by K. Huttinger,

Universitat Karlsruhe, West Germany. More than 400,000 components for heart valves have been implanted. Isotropic carbon and carbon-silica carbide composites are used, respectively, for hip joint cups and balls. The stem of the hip joint is fabricated from a carbon-fiber-reinforced carbon composite. New research has shown that for the first time tendons and ligaments can be repaired with the use of carbon fiber strands and fabrics, which provide strength for the new tendon and a substrate for new tissue growth.

PRODUCTS

New carbon products described in a poster session included a fine carbon-carbon composite for pencil lead that could be shaped as a spring with good elasticity (Mitsubishi Pencil Company, Ltd.), a high-quality needle coke with low thermal expansion (Koa Oil Company), large-sized, isotropic graphites of high-density and high-strength for nuclear, metallurgical, and electrical applications (Toyo Tanso Company) impervious graphite and carbons for electrodes for electrical discharge machining (Toyo Carbon Company), a high-density, high-strength graphite (Tohoku-Kyowa Carbon Company) and inexpensive silicon-carbide whiskers (Tokai Carbon Company). These carbon products highlight the innovative and advanced research on carbon and graphite being conducted by many universities and companies throughout Japan.

DISCLINATIONS IN A GRAPHITE-FIBER BUNDLE

J. E. Zimmer and R. L. Weitz
Acurex Corporation, P.O. Box 7555, Mountain View, California 94039

With its unique properties, graphite has application as a high-temperature, structural material and a biocompatible material for prosthesis. At the same time, graphitic materials are one of the few materials that contain disclinations and for which disclinations are of practical importance. Disclinations¹ exist in graphite-fiber reinforced, graphite-matrix composites. For those carbon-carbon composites with matrix formed from the carbonaceous mesophase, a discotic nematic liquid crystal, disclinations are abundant and can be expected to play a role in the fracture behavior of these composites. We present here, as a first step to understanding this fracture behavior, the identification and characterization of the disclinations in a graphite-fiber bundle. The fracture behavior of the graphitic matrix has been shown previously to be affected by disclinations².

Optical micrography has been used to identify the disclinations in the graphite-fiber bundles. Composites of Hercules HM polyacrylonitrile-based, graphite fiber and Ashland A240 petroleum pitch were carbonized to 600°C. Specimens were sectioned transverse to the fiber bundles, polished, and observed under immersion oil with cross polarized light. Structural sketches of the matrix along the fibers were made by tracing on an overlay on the micrograph the orientation of the mesophase layers underlying the extinction contours. This was done for micrographs at various angles of rotation of the crossed polarizers to map the entire matrix region.

Negative wedge disclinations exist among the filaments in a fiber bundle as shown in Figures 1 through 4. Two features prescribe the type of disclinations present. First, the disk-like molecules of the mesophase tend to align parallel to the surface of the graphite filaments, forming a circular sheath several microns in thickness about each filament. The parallel alignment of the filaments and the mesophase sheath force the disclination lines to be parallel to the filaments. Second, the local arrangement or pattern of the arrays of filaments determines the strength and type of disclination. The strength of a disclination is a measure of the rotational distortion associated with the disclination. The type of disclination for each filament array is summarized in Table 1. Normally, disclinations of strength higher than 1 are not observed in bulk mesophase as the high-strength disclinations readily disassociate to lower-strength disclinations. (The energy of a disclination is proportional to the square of its strength.) Reported here is the first evidence of disclinations of higher strength in the carbonaceous carbonaceous mesophase. Concurrently, evidence for high-strength disclinations in a conventional nematic liquid crystal has been obtained³.

Analysis of the structure of the core of these disclinations has aided their classification. The disclinations of strength $S = -1/2$ and $S = -3/2$ have discontinuous cores. In a discontinuous core, the configuration of the molecules on the plane perpendicular to the disclination line is retained to the center of the disclination. Any tilting of the molecules is not allowed topologically. The disclinations of strength $S = -1$ and $S = -2$ have continuous cores where the parallel alignment of the molecules is retained throughout the core by tilting of the molecules out of the plane of the disclination. These continuous cores are saddle shaped, as shown in Figure 5. The optical micrography has indicated that the mesophase layers are indeed perpendicular to the disclination line at its center.

Support by the Office of Naval Research is gratefully acknowledged.

¹J.E. Zimmer and J.L. White, *Advances in Liquid Crystals* 5 (1983) 157.

²J.E. Zimmer, International Symposium on Carbon, Extended Abstracts, Toyohashi, Japan, 1-4 November 1982, 131.

³N.V. Madhusudana and R. Pratibha, *Current Science* 51 (1982) 877.

Table 1. Disclinations in Filament Arrays

Array	Strength of Disclination	Number of Extinction-Contour Arms	Structure	Relative Energy
Triangular	-1/2	2	Discontinuous	1
Square	-1	4	Continuous	4
Pentagonal	-3/2	6	Discontinuous	9
Hexagonal	-2	8	Continuous	16

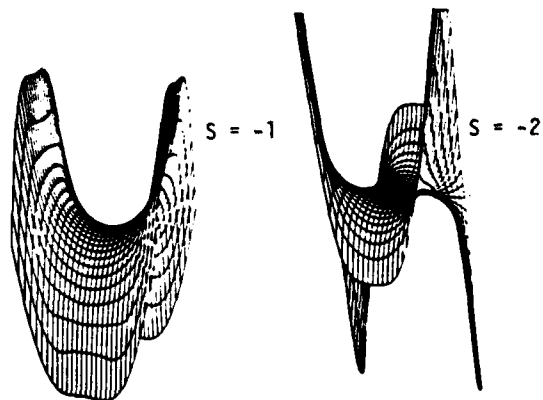


Figure 5. Saddle-shaped surfaces representing orientation of molecules in continuous cores

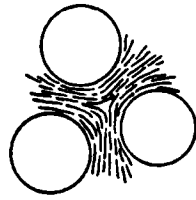
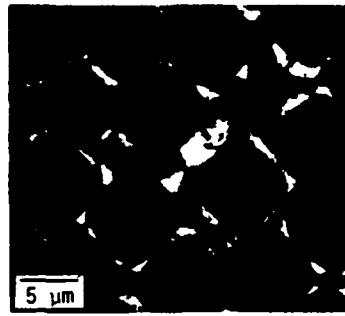


Figure 1. Disclination of strength $S = -1/2$ in triangular array

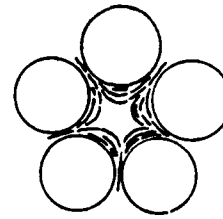
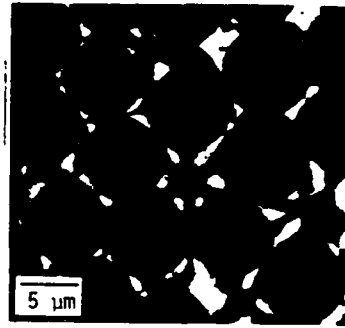


Figure 3. Disclination of strength $S = -3/2$ in pentagonal array

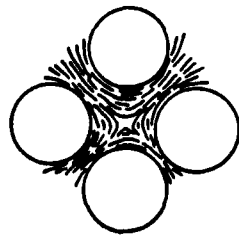
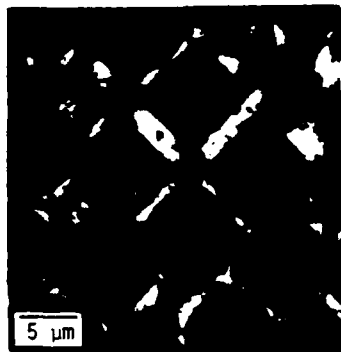


Figure 2. Disclination of strength $S = -1$ in square array

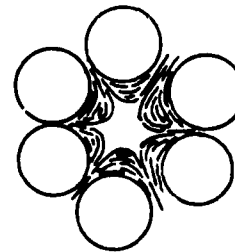
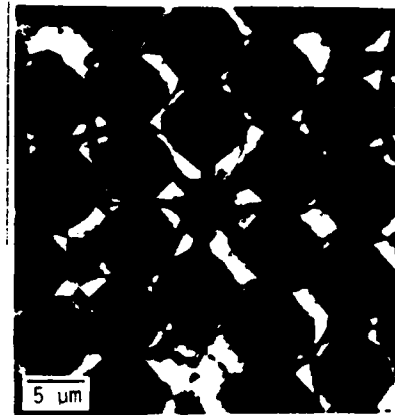


Figure 4. Disclination of strength $S = -2$ in hexagonal array

REFERENCES

1. J. D. Brooks and G. H. Taylor, Chem. and Phys. of Carbon 4, 243 (1965).
2. J. L. White, Progr. in Solid State Chem. 9, 59 (1975).
3. J. L. White and J. E. Zimmer, Surface and Defect Properties of Solids 5, 16 (1976).
4. I. Mochida, K. Maeda and K. Takeshita, Carbon 16, 459 (1978).
5. J. E. Zimmer and J. L. White, Advances in Liquid Crystals 5, 157 (1982).
6. F. R. N. Nabarro, Theory of Crystal Dislocations, Clarendon Press, Oxford (1967).
7. V. Volterra, Ann. Sci. Ecole Norm. Super., Paris, 24, 401 (1907).
8. J. L. White, G. L. Guthrie, and J. O. Gardner, Carbon 5, 517 (1967).
9. J. E. Zimmer and J. L. White, Mol. Cryst. Liq. Cryst. 38, 177 (1977).
10. J. L. White and J. E. Zimmer, Carbon 16, 469 (1978).
11. J. E. Zimmer, Ph.D. Thesis, Purdue University, 1978.
12. J. E. Zimmer and R. L. Weitz, Technical Report TR-82-24/ATD, Acurex Corporation, September 1982.
13. M. Buechler, C. B. Ng, and J. L. White, Extended Abstracts, 15th Conference on Carbon, p. 182 (1981).

END

FILMED

1-84

DTIC